UNIVERSITÀ DEGLI STUDI DI PADOVA

DIPARTIMENTO DI INGEGNERIA CIVILE, EDILE E AMBIENTALE

CORSO DI LAUREA MAGISTRALE IN ENVIRONMENTAL ENGINEERING

HYDRODYNAMIC MODELLING OF URBAN AREAS

ANALYSIS OF KEY FEATURES AND DEVELOPMENT OF A NEW, ANISOTROPIC ARTIFICIAL POROSITY, SUBGRID MODEL

Relatore: Ch.mo Prof. Ing. Andrea Defina

Correlatore: Ing. Daniele Pietro Viero

Laureando: Francesco Ballarin

Matricola: 1057831

Anno Accademico 2014-2015

Un ringraziamento particolare al Prof. Andrea Defina per la sua disponibilità e all'ing. Daniele Pietro Viero per avermi accompagnato nella realizzazione di questa tesi. Ringrazio inoltre tutta la mia famiglia e gli amici che mi hanno sempre sostenuto durante questi anni.

Abstract

Recent flood events occurred in Italy reveal a diffuse hydraulic vulnerability. Moreover, due to the diffuse urbanization of the Italian country, flooding hazard often involves areas that are densely populated. In this context, a fundamental aspect is the development of suitable mathematical hydrodynamic models, able to face properly hydraulic hazard. In particular, the simulation and the analysis of flood events in urban areas is a challenging task for a number of reasons, as the complex geometry of cities and the presence of a large number of obstacles of various shapes and length scales. These features affect water storage capacity, as well as the dynamic of inundation processes and the final extension of flooded area. Moreover, this is a crucial application area: potential flood damages in urban areas are actually greater than in rural areas and urban flood inundation receives a relatively high political profile.

The first part of the thesis is an analysis aiming at identifying the key features that significantly affect the flooding dynamics in urban areas. The potential effects of small-scale features, which commonly characterize urbanized districts, are investigated by applying relatively small changes to model geometry. The effects of these diverse modelling choices on the prediction of inundation extent, flow depth and velocity are analyzed. Far from being a simple model sensitivity analysis, general conclusion can be drawn about management of urban areas, since the geometry variations here applied are

consistent to minor changes that could commonly occur in generic urban areas (e.g. garden walls, sidewalk, etc.). All these aspects have to be carefully considered by modelers before carrying out any modelling exercise in urbanized area. Suitable decision have to be made according to the specific purpose of modelling studies (e.g., real-time prediction or ex-post analysis, high-resolution or catchment-scale applications, interventions planning or flood hazard mapping, etc.).

The second part of the thesis deals with the macroscopic simulation of urbanized areas, by means of subgrid modelling techniques. Different subgrid approaches have been analyzed, which account for urban topographical features that are too small to be explicitly reproduced in the context of, e.g., catchment-scale applications. Particularly, a novel approach is developed and tested, which is based on the concept of artificial porosity and on an anisotropic formulation of the shallow water equations. The parameters needed by the model are physically meaningful: therefore, they are easy to be a-priori inferred from geometrical, topographical information. Application of the proposed approach is straightforward, and the obtained results seem promising.

Table of contents

1 Introduction

Recent flood events occurred in Italy reveal a diffuse hydraulic vulnerability. Moreover, due to the diffuse urbanization of the Italian country, flooding hazard often involves areas that are densely populated, causing huge economic damages. Considering only the last years, several flood events occurred, affecting urban areas: Genova (2014-2011), Carrara (2014), Parma (2014), Chiavari (2014), Sardegna (2013), Cinque terre (2011) and Veneto (2010). In addition, less recent but well-known and extremely devastating flood events involved urban areas as Genova (1970) and Firenze (1966). Starting from these considerations, a modern and accurate modelling of the hydraulic processes that led to these (or similar) disasters can certainly improve the management of hydraulic hazard in urban areas.

In this context, a fundamental aspect is the development of suitable mathematical hydrodynamic models, able to face properly hydraulic hazard. Mathematical models are widely used for solving hydraulic problems. In the past, mainly one-dimensional models were used to simulate flood propagation, essentially due to their simple implementation. This approach results, in some applications, too restrictive. Some fundamental assumptions, used to derive one-dimensional equations, are often not verified, thus leading to deluding, unrealistic results. Fluvial flooding models require prediction of flows over complex topography and the flow routing over floodplains is known to be highly two-dimensional (Yu and Lane 2006).

Recently, also thanks to higher computing power, two-dimensional models were developed in order to provide more reliable results. Two-dimensional models are able to simulate flood events in wide areas in case of uncontrolled discharge and describe more accurately flood waves propagation in wide riverbeds. By flood events, the model equations and the computational domain needs to be adjusted considering the non-negligible effects that different structures, present in the area, cause to flood propagation.

Two-dimensional inundation models have been developed and shown to provide good predictions of flood inundation extent (Yu and Lane 2006, McMillan and Brasington 2007, Guinot 2012). Moreover, two-dimensional models can simulate accurately the local pattern and timing of floodwater depth and flow velocity (McMillan and Brasington 2007). These models can be used also to help planning mitigation measures in rural or urban areas, enabling informed flood risk zoning and improved emergency planning (McMillan and Brasington 2007, Mignot 2006). Mathematical hydrodynamic models, solving shallow water equations over two-dimensional domains (i.e., De Saint Venant equations), are now commonly used tools. Two-dimensional models are widely applied to investigate complex hydrodynamic problems, in both environmental and artificial contexts.

In the last decade, high-resolution terrain data surveys were increasingly used to support two-dimensional flood inundation modelling researches (McMillan and Brasington 2007). High-resolution data, obtained from airborne remote sensing, increase opportunities for representation of small-scale structural elements in complex floodplain systems.

These new topographic data sources, which can yield synoptic information at a resolution that in many cases is better than 2.0 m and a precision that is better than 0.15 m, provide new opportunities for modelling floodplain inundation. The presence of different structures on a river floodplain is important concerning the volume that cannot be occupied by water (storage reduction), and to flow velocities (both the modulus and the direction) (Yu and Lane 2006).

In particular, the simulation and the analysis of flood events simulation in urban areas is a challenging task for a number of reasons: presence of a large number of obstacles of various shapes and length scales, buildings storages capacity and cities complex geometry (Mignot 2006, Schubert 2008, Guinot 2012). Surface flood modelling in urban environment requires explicit representation of small-scale topographic features in order to capture the correct local patterns of flux near structural elements. These structures also determine a sort of blockage effect due to particular topographical features, which create continuous obstacles to flow propagation and produce major effect on flow routing process (Yu and Lane 2006, Guinot 2012).

Moreover, this is a crucial application area; potential flood damages in urban areas are actually greater than in rural areas and urban flood inundation receives a relatively high political profile (Yu and Lane 2006). Simulation of flooding scenarios is necessary to assess hydraulic hazard. Additionally, to implement risk-based flood mitigation, consequences of flood hazard must be quantified in terms of property damages, ecological damages, health damages and other social effects (Schubert 2008, Sanders 2008).

In this thesis is applied a model called 2DEF, whose detailed description is reported in Appendix A. Built by University of Padova researchers, 2DEF is continuously been developed to implement new features. 2DEF is a 2D-1D coupled model that implements an original technique to simulate wetting and drying transition, as described in Appendix B.

The first part of the thesis is an analysis aiming at identifying the key features that significantly affect the flooding dynamics in urban areas. Attention will be paid in order to highlight the model sensitivity to geometrical and topographical variations. The potential effects due to small-scale features, which commonly characterize urbanized districts, are investigated by applying relatively small changes to model geometry. The effects of these diverse modelling choices are analyzed on the prediction of inundation extent, flow depth and velocity (Guinot 2012). Far from being a simple model sensitivity analysis, general conclusion can be drawn about management of urban areas, since the geometry variations here applied are consistent to minor changes that could commonly occur in generic urban areas (e.g. garden walls, sidewalk, etc.). All these aspects have to be carefully considered by modelers before carrying out any modelling exercise in urbanized area. Suitable decision have to be made according to the specific purpose of modelling studies (e.g., real-time prediction or ex-post analysis, high-resolution or catchment-scale applications, interventions planning or flood hazard mapping, etc.).

In the second part of the thesis, flooding of urban areas is deal with from a quite different perspective. One of the main challenges is, indeed, how to extend process-based models, which can naturally consider detailed aspects of building geometry, to the catchment scale (Sanders 2008). The fundamental issue is that meshes at the catchment scale, due to computational limits, can only solve features considerably larger than small-scale structural elements. Consequently, subgrid models have been developed and applied to account for topographic variability that is too small to define with a catchment-scale mesh but is important for flood events representation (McMillan and Brasington 2007, Sanders 2008, Guinot 2012).

To this aim, different subgrid models are tested and analyzed. Schematic applications are performed for verification purpose. Attention is paid to: i) test model ability to resolve the main flow field characteristics and, particularly, the preferential flow directions; ii) verify the physical basement (and thus the practical applicability) of the approach; iii) take a look at the requested computational resources.

The first approach make use of 2D special elements already implemented in the 2DEF model, which allows macroscopic simulation of urban areas. Such two-dimensional elements accounts for buildings presence and obstacles in terms of both reduced water storage and increased flow resistance. A detailed description of these special elements is reported in Appendix C.

In the second approach, we apply another feature that was already implemented in 2DEF, initially developed to deal with anisotropic flow resistance in rural areas, where networks of minor channel, such as ditches and furrows, produce non-negligible anisotropic effect on flow directions. The user has to specify the values of roughness parameters along the two principal direction, along with the rotation angle of principal axes with respect to the x-y reference of the computational mesh. The effects exerted on the flow field by buildings or preferential pathways are modelled through suitable resistance parameters, which in fact are clearly conceptualized in this approach.

The third method is developed and tested for the first time in this thesis and is a completely new approach for a subgrid model in urban area. This new approach applies an artificial porosity in the two main flow directions. This porosity is calculated as the ratio of the width available to water flowing to the total width of the urban area. This artificial porosity consider the global resistance of the urban area and simulate the presence of preferential pathways.

The different approaches here investigated are then discussed singularly to highlight their advantages and limitations, also accounting for the conclusion drawn in the first part of the thesis.

A set of conclusions closes the thesis.

2 Effects of high-resolution features in urban areas

2.1 Introduction to the problem

Starting from a real urban area, a model is created to perform high-resolution simulation of urban flooding. The real urban area can be assumed representative of a generic urban area, with a largely anisotropic structure. The main goal is to assess the blockage effects of walls and buildings in the propagation of flood waves and in the extents of flooded areas.

A specific area is isolated from external region making it independent from real outside conditions. Therefore, the model does not represent an actual urban area but maintain the principal geometrical characteristic of a real one. From a real urban area, highlighted by a red line in Figure 2.1 (page 10), are extracted the houses location, the streets direction and the position of gardens wall. External area is not included in the simulation and it is supposed to be very regular.

Figure 2.1 Portion of a real urban area, used in the numerical investigation. (www.google.it/maps)

This chapter aims at investigating how high-resolution features inside an urban area affect the simulation results, in terms of flooded areas, flow direction and velocity. Analyzing the characteristic of a generic urban area, the walls presence around gardens (i.e., along the streets) seems to play a crucial role.

In the Figure 2.2, at page 11, is possible to notice that concrete walls around gardens have different heights and gates opening. The walls height is, in first approximation, comparable to the probable water depth during a flood event so become relevant to calculate these heights in order to determine the propagation of flood wave inside the urban area. Wall characteristic (i.e., location, elevation and openings) could not be measured manually in complex or wide area; neither airborne remote sensing allow capturing them, due to the limited width of the walls and to the presence of vegetation (Figure 2.2). This type of construction is not fixed and can be modified during quite common houses maintenance. This means that also a very accurate model, from a topographic point of view, could become ineffective after few years. In conclusion, the aim of this chapter is to investigate the influence of high-resolution structures (particularly garden walls) on flood propagation in the view of hydraulic hazard assessment inside an urban area.

Figure 2.2 Concrete wall representation inside an urban area (www.google.it/maps)

2.2 Urban area schematic application

First, different sets of computational elements are created to simulate the urban area in different ways. Elements geometry is chosen in order to analyze the importance of wall presence starting from the same initial topographical information. This characterization progressively considers and analyzes the presence of walls.

The first simulation created, called NO_WALL, do not consider the presence of walls. A second simulation is made considering the height of concrete walls equal to 0.2 m, called 0.2_WALL. A third simulation is prepared considering the height of concrete wall equal to 0.4 m, called 0.4_WALL. Finally, the last simulation is made with no possibility for water to overcome the walls, which is equivalent to model the urban area as a grid of streets, called STREETS_GRID.

Figure 2.3 report, for the same area, the different computational grids. The first image, where only the presence of houses can be identified, refers to the NO_WALL model. The second image refers to 0.2_WALL and 0.4_WALL models: small triangular elements used to simulate the presence of walls around houses are visible. Last image refers to the STREETS_GRID model: in this case, houses and gardens are excluded and result not floodable.

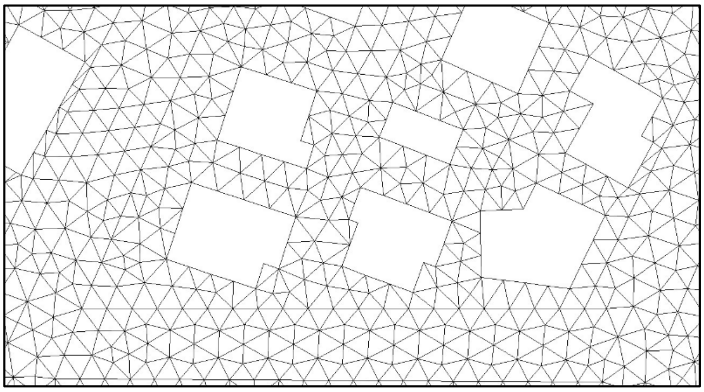

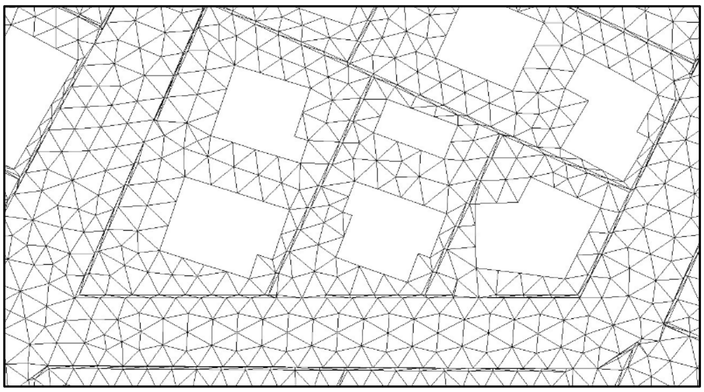

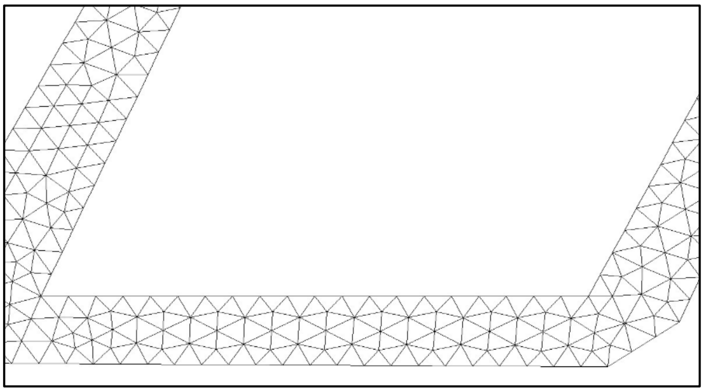

Figure 2.3 Different computational grids for the same portion of urban area.

All parameters used for different simulation are reasonably assumed in order to simulate a typical urban area. Bottom slope is set constant and equal to 0.65‰ for describe an urban area in lowland environment, as the one shown in Figure 2.4.

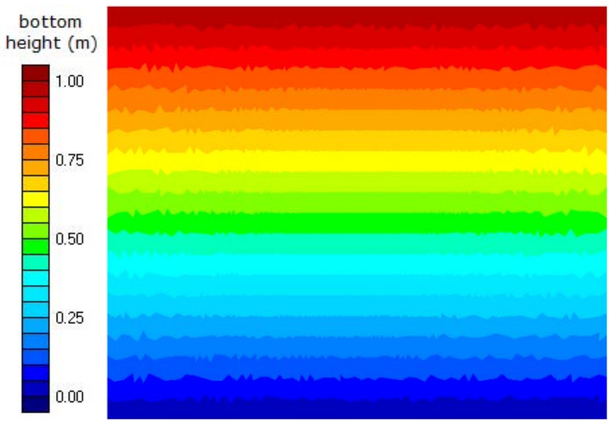

Figure 2.4 Model slope representation

The hydrodynamic model 2-DEF model make use of the Gauckler-Strickler formulation to model the bottom friction, and the parameter k_s has to be specified for every computational element. In the model, this parameter is set equal to 65 [$m^{1/3}s^{-1}$] for streets and equal to 35 [$m^{1/3}s^{-1}$] for gardens and outside area. (Figure 2.5)

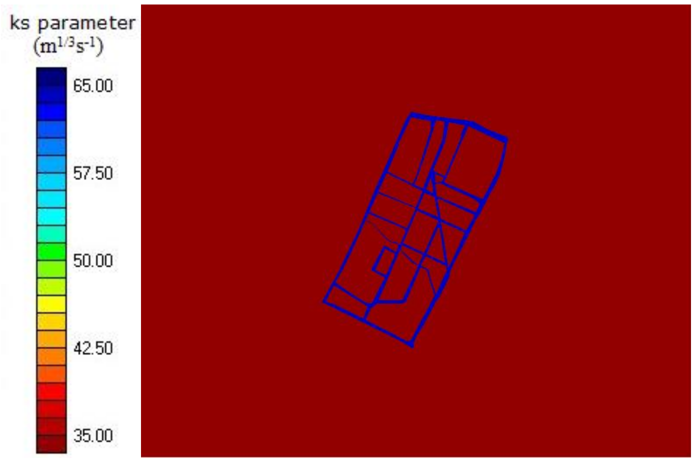

Figure 2.5 Bottom roughness representation

The parameter a_r, which is a measure of the typical height of bottom macro-roughness, is assumed equal to 0.1 m and constant everywhere. This parameter plays a key role in simulating the wetting and drying processes (see Appendix B for a more detailed description).

The simulation time is choose sufficiently long (5 hours) in order to reach steady state conditions.

The discharge select permit the transition from dry to wet conditions of soil in adequate time. At the lowest edge of the mesh, a properly dimensioned 1D-channel collects all the discharge.

The calculation timestep is set as larger as possible in order to reduce the computational burden and, at the same time, to provide stable numerical solutions. In models NO_WALL and STREETS_GRID, due to their relative simplicity, a 2 s timestep is used. Otherwise, for the 0.2_WALL and the 0.4_WALL models, a 0.2 s timestep is used, due to the reduced dimensions of the grid elements.

2.2.1 Schematic model application

The results of different simulation are reported in term of velocity and water depth. All the images refer to steady state conditions achieved at the end of the simulations. The same chromatic scale is used in the subsequent images, for both water depth and velocity analysis, so it is possible to compare the results for the different scenarios.

- NO_WALL model

In this model, as reported before, elements representing a house's areas are eliminated. The garden walls around the houses are completely ignored so all the gardens result completely and immediately floodable. Figure 2.6 and Figure 2.7 report the results for the NO_WALL model.

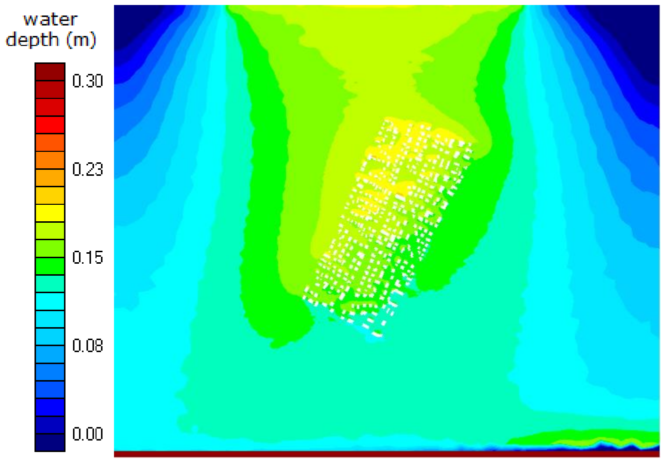

Figure 2.6 Water depth distribution for NO_WALL model

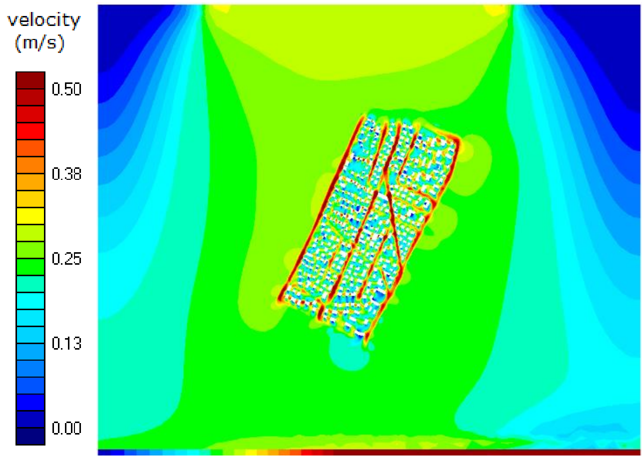

Figure 2.7 Velocity distribution for NO_WALL model

The water depth distribution in Figure 2.6, allows identifying the additional resistance caused by the urban area due to buildings presence (yellow area). The anisotropic distribution of houses determines higher levels in the upper-left zone. The velocity distribution, in Figure 2.7, reveals that higher values occur along the streets due to the minor roughness (i.e., lower bottom friction): consequently, streets behave as preferential pathways. Lower values of velocity are located behind buildings due to their shadow effect (see the particular in Figure 2.8).

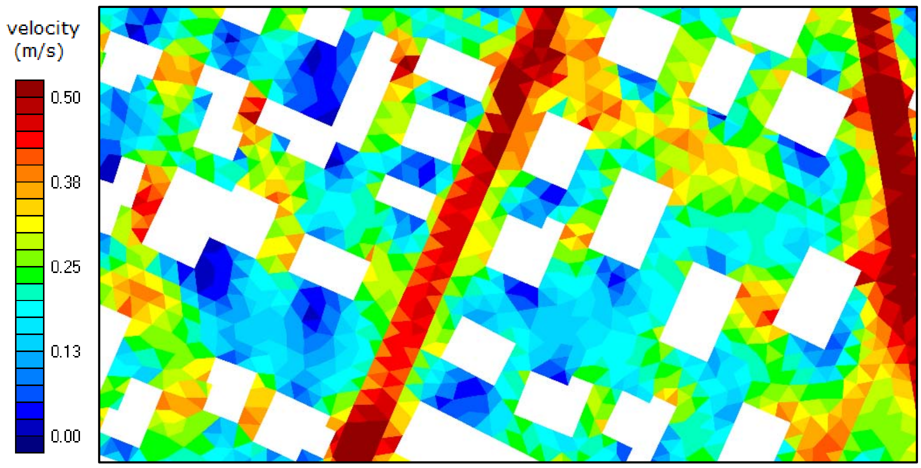

Figure 2.8 Velocity distribution zoom in NO_WALL model

- 0.2_WALL model

Computational elements covering the house's areas are excluded from the mesh, as for the NO_WALL model. In addition, 0.2 m high walls around houses are modeled and interrupted in some sections to simulate the presence of gates. As a result, gardens results floodable only if water rises over these structures or by entering through the gates. Figure 2.9 and Figure 2.10 report the results for this model.

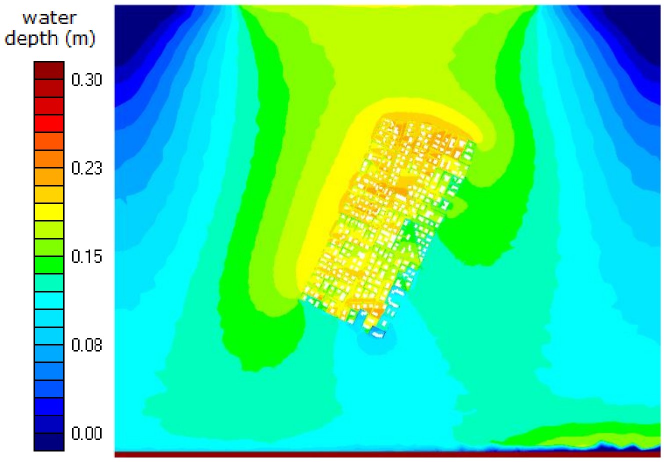

Figure 2.9 Water depth distribution for 0.2_WALL model

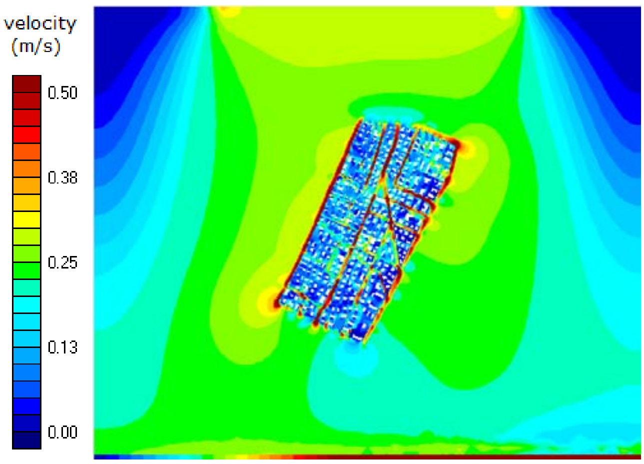

Figure 2.10 Velocity distribution 0.2_WALL model

Considering the presence of walls in the modeled area, also if relatively small (20 cm), completely change the simulation results, as one cannot by comparing the water depth distribution referring to the NO_WALL and 0.2_WALL models (Figure 2.6 and Figure 2.9, respectively). The global resistance in 0.2_WALL model increase due to the walls, as shown by higher water depths in the upper-left corner of the urbanized area (light orange area in Figure 2.9) and flow clearly deviate toward left side. The anisotropic effect of the area is here more evident. The water depth inside gardens areas is strongly affected by the position of walls and gates opening. In Figure 2.9, which shows the water depth distribution, is possible to notice neighboring garden with significantly different water depth (from orange to blue), indicating the fundamental effects of wall.

Walls also modify the distribution of flow velocity field inside the urban area. Velocity is maximum along streets with local values up to 1 m/s. On the contrary, in the garden velocity is minimum also if completely flooded (compare Figure 2.11 with Figure 2.8).

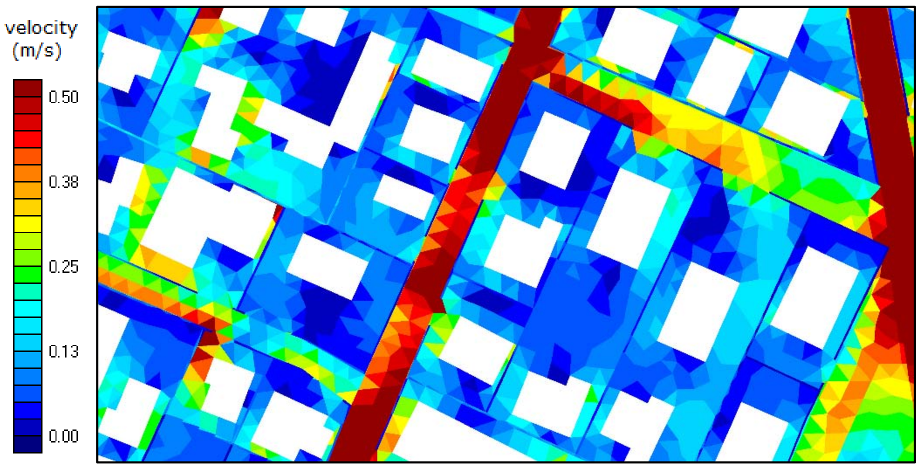

Figure 2.11 Velocity distribution zoom in 0.2_WALL model

- 0.4_WALL model

In analogy with models 0.2_WALL, every element inside the house's areas is excluded from the computational mesh. The garden walls are modeled by increasing their bottom elevation of 0.4 m, interrupted in some sections to simulate, the presence of openings.

Every garden results floodable only if flow overcome these structures or enters the gates. All other model parameters, like roughness parameter and water discharge, are the same of the previous cases. Figure 2.12 and Figure 2.13 reports the results for this model, in terms of water depth and flow velocity, respectively.

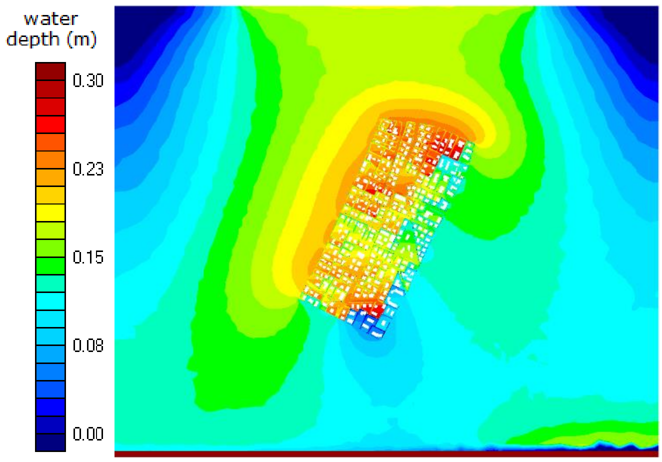

Figure 2.12 Water depth distribution for 0.4_WALL model

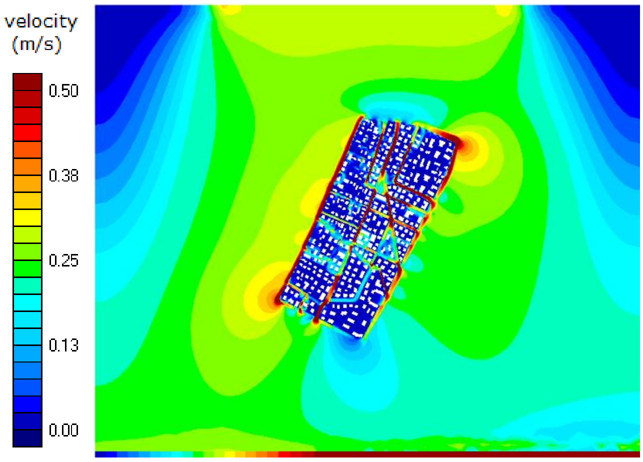

Figure 2.13 Velocity distribution for 0.4_WALL model

Increasing walls height, the characteristics described from the model 0.2_WALL are maintained but increased in magnitude.

The global resistance and the asymmetry of the flow due to buildings and walls increase from the previous case (orange area in Figure 2.12).

Water depth inside the garden areas depend on the position of walls and gates opening. In Figure 2.12, which shows the water depth distribution, is possible to notice neighboring garden with different water depth (from red to blue) indicating the fundamental effects of walls.

The Figure 2.14 reports a detailed image of water depth distribution highlighting the walls influence inside gardens.

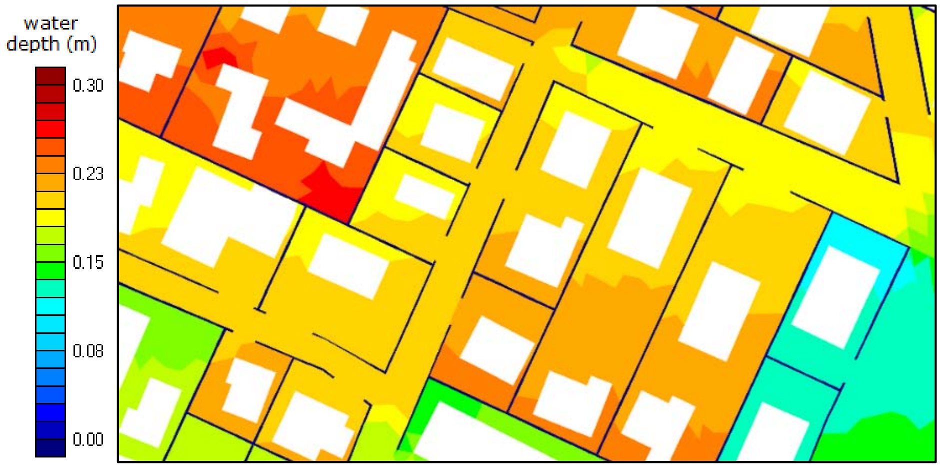

Figure 2.14 Zoom showing water depth distribution in 0.4_WALL model

Flow velocity inside gardens is near to zero even if gardens are completely flooded. This mean that gardens behaves as storage areas, while only the streets actively participate to the passage of water (compare Figure 2.15 with Figure 2.8 and Figure 2.11).

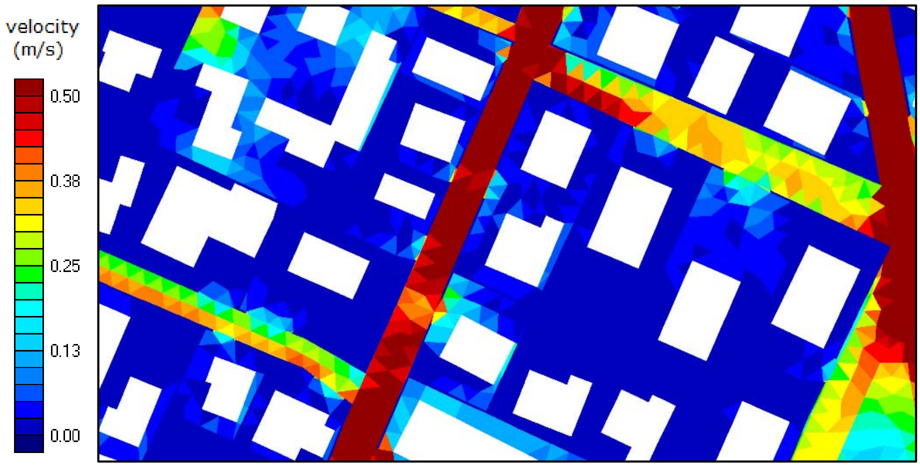

Figure 2.15 Zoom showing velocity distribution in 0.4_WALL model

- STREETS_GRID model

In this scenario, elements representing house and gardens are both excluded from the mesh. All gardens results completely not floodable so gardens areas are completely external to water flow and consequently to water storage. Model parameters, like roughness parameter and water discharge, are the same of the previous cases. Figure 2.16 and Figure 2.17 report the results for this model, in terms of water depth and flow velocity, respectively.

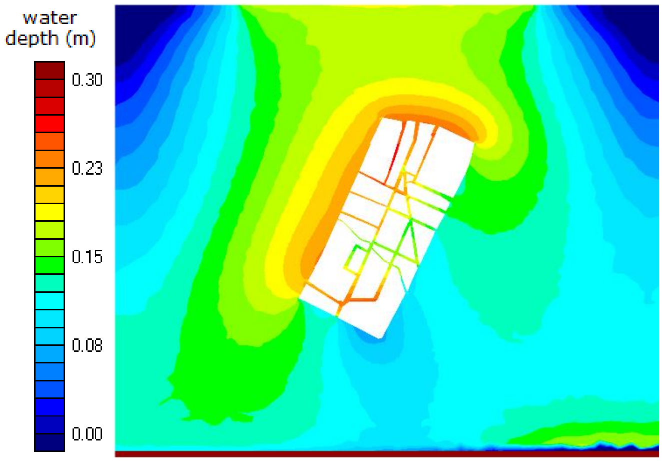

Figure 2.16 Water depth distribution for STREETS_GRID model

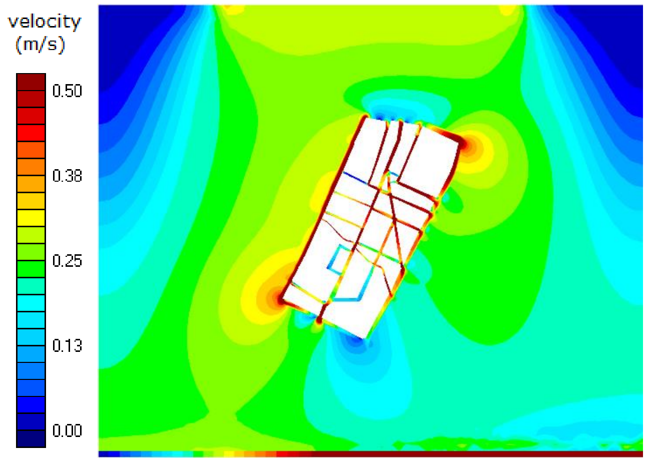

Figure 2.17 Velocity distribution for STREETS_GRID model

Modelling the urban area as a network of streets is equivalent to the indefinitely increasing of the walls height. Water depth and velocity along the streets are comparable to those of 0.4_WALL model (Figure 2.12 and Figure 2.16 for water depth distribution and the Figure 2.13 and Figure 2.17 for velocity distribution).

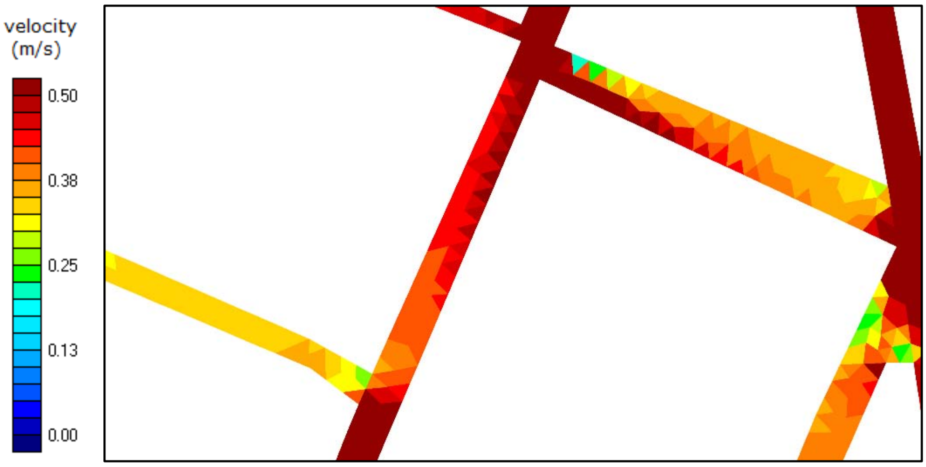

Figure 2.18 Zoom showing velocity distribution in STREETS_GRID model

2.3 Comparison under time varying conditions

Numerical simulation under time varying conditions are here considered, to better analyze the effects of high-resolution features in urban areas and how structures affect both paths and celerity of a flood wave. The following Figure 2.19 represents the inflow hydrograph over the simulation time.

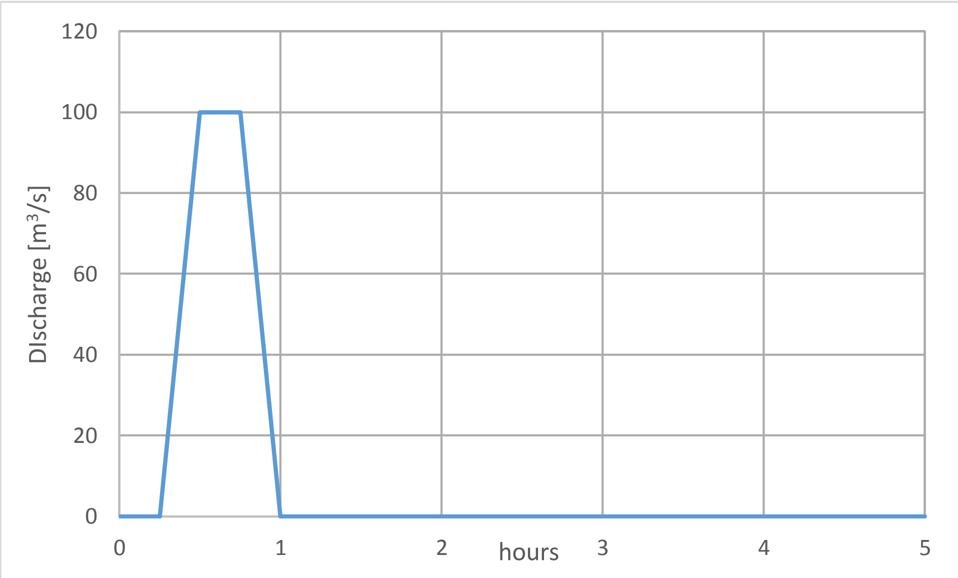

Figure 2.19 Inflow hydrograph used in time varying simulations

The water depth distribution at t=40, 60 and 240 min, for the different models previously considered, is reported in order to highlight differences and similarities (Figure 2.20, Figure 2.21 and Figure 2.22.)

At t=40 min, the discharge reaches its maximum value (Figure 2.19) and the water front is inside the urban area. Depending on the model utilized, different propagation speeds and water depths can be noticed (Figure 2.20).

In the 0.2_WALL model the water front is locally blocked by walls, which create a heterogeneous distribution of water depth and a slower propagation speed. In the STREETS_GRID model, the water is deeper in the upper part of the urban area, due to the impossibility of water flow to overcome the walls. Moreover, in the STREETS_GRID model, the water depth on the streets is larger and the water front propagate more rapidly due to the lack of storage areas for water (e.g. gardens).

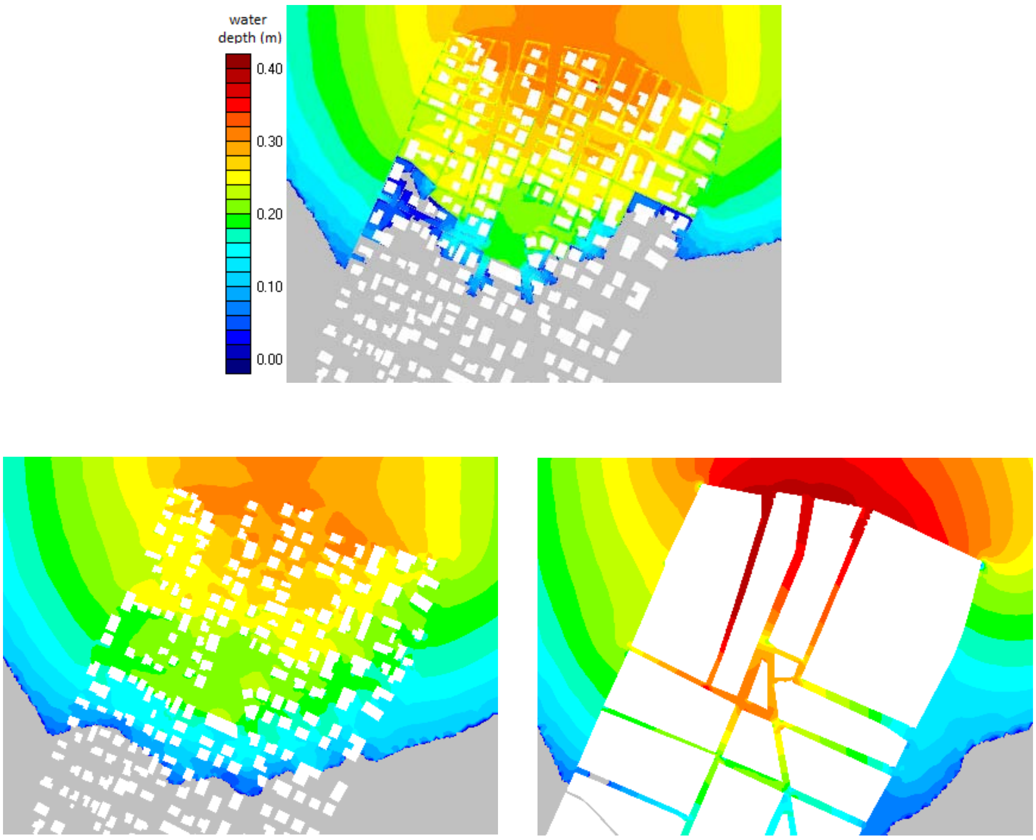

Figure 2.20 Water depth distribution at t=40 min: 0.2_WALL (top), NO_WALL (left) and STREETS_GRID (right) models

At t=60 min, the water front is completely inside the urban area and the upstream inflow is equal to zero (Figure 2.19).

Once again, analyzing the Figure 2.21, the water depth in 0.2_WALL model is characterized by a heterogeneous and locally variable behavior with respect to the NO_WALL model. In the 0.2_WALL model the flooded area is smaller in particular with respect to the STREETS_GRID model, where the streets convey the flow more rapidly in the entire urban area.

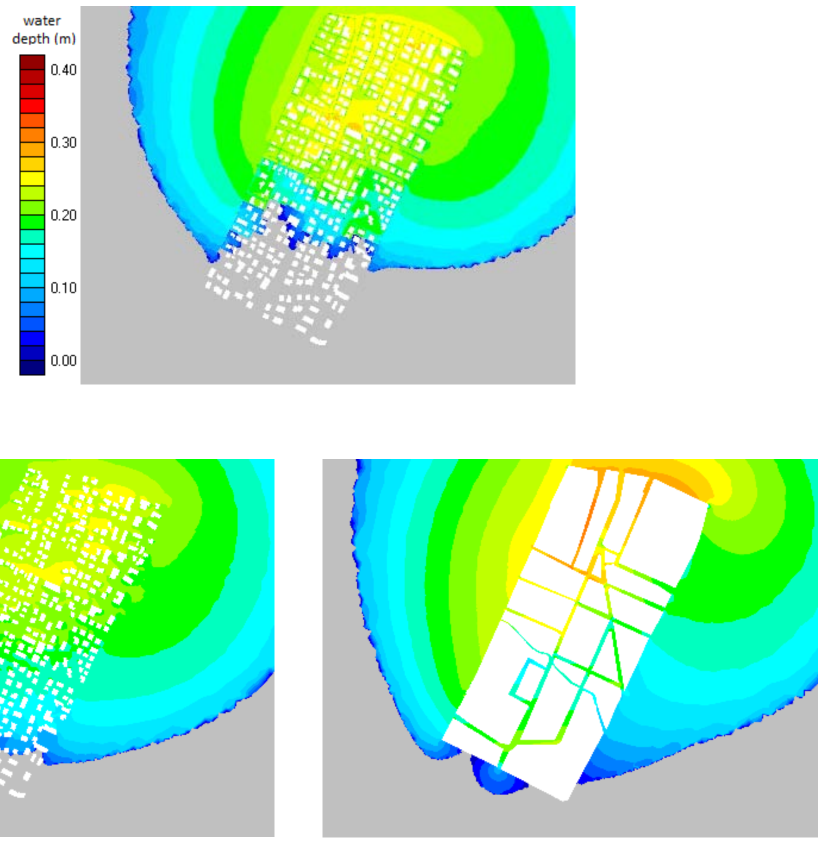

Figure 2.21 Water depth distribution at t=60 min: 0.2_WALL (top), NO_WALL (left) and STREETS_GRID (right) models

The last comparison, which refers to t=4h, allow us to analyze how the flood wave exits from the urban area and how much water remains stored within the urban area (Figure 2.22).

As expected, in the 0.2_WALL model, the water is blocked in garden areas by the walls and remains inside the urban area for a longer time. In the STREETS_GRID and NO_WALL models, on the contrary, the regular disposition of houses and streets, and the absence of garden walls, let the flood exit more rapidly.

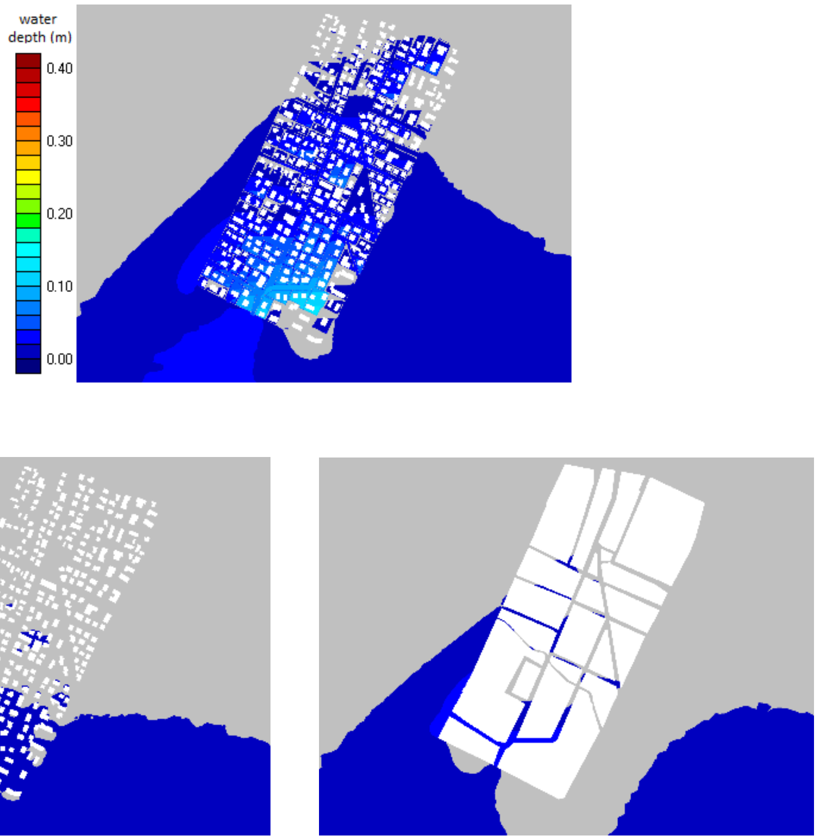

Figure 2.22 Water depth distribution at t=240 min: 0.2_WALL (left), NO_WALL (center) and STREETS_GRID (right) models

A local analysis is carried out for a point located on a street. Figure 2.23 and Figure 2.24 report the trend of the specific flow rate and the water. In the STREETS_GRID model, the specific flow rate increases rapidly, reaches larger values, and rapidly decrease (Figure 2.23), due to the absence of lateral storage areas (i.e., gardens). Moreover, the values of specific flow rate and water depth increase earlier, with respect to other models, thus confirming the faster flood propagation in the STREETS_GRID model.

In the NO_WALL and 0.2_WALL models, the maximum value of specific flow rate and water depth is smaller due to the larger available floodable areas (gardens). The consequence of water storage is evident also considering the tail of the graphs in Figure 2.23 and Figure 2.24: the water depth and the specific flow rate in the 0.2_WALL are initially smaller than in the STREETS_GRID, but after the peak, they become larger. This is due to the water previously stored in gardens and then slowly released.

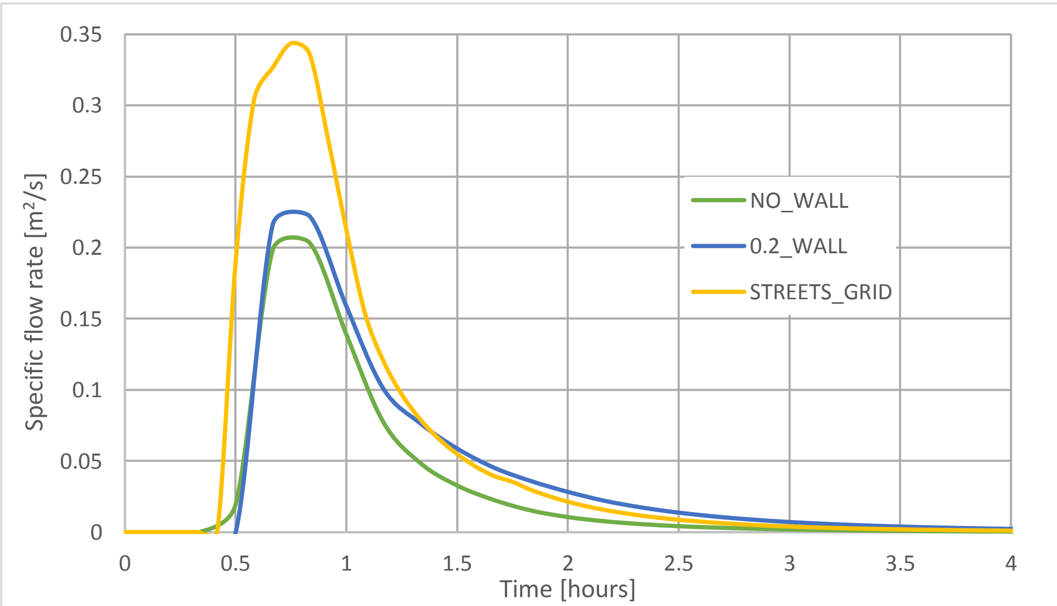

Figure 2.23 Specific flow rate in a point located on a street, for the three different models considered

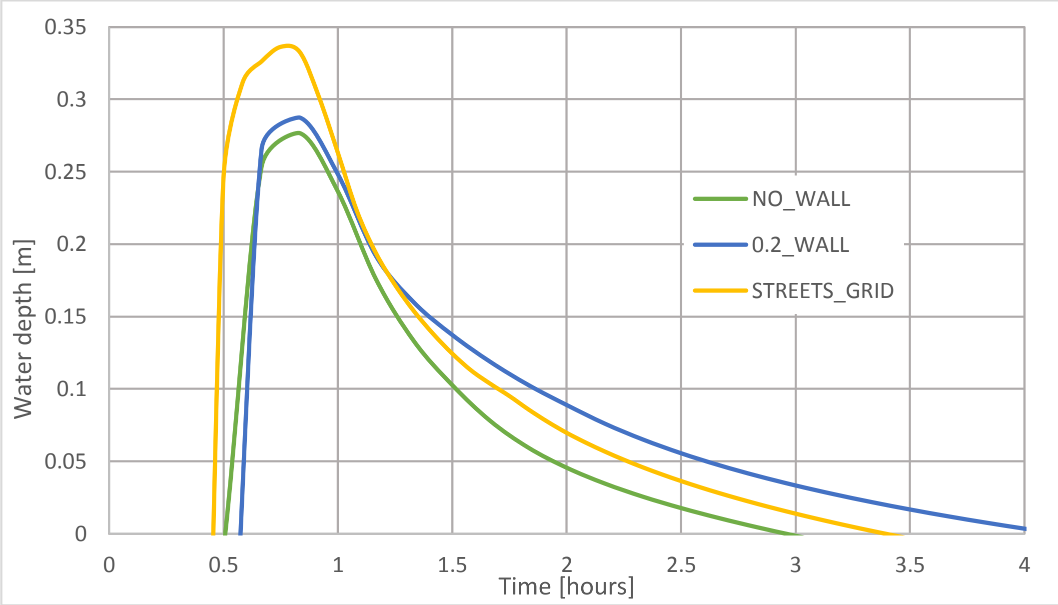

Figure 2.24 Water depth in a point located on a street, for the three different simulation considered

2.4 Discussion

Analyzing the different models presented in the previous subsections, it is evident that also little variations in the topography of urban areas can produce significant effects on flooding. Small variations in position and height of garden walls or gates produce non-negligible effects on flooded area extension and on the flow field, in terms of both water depth and velocity. This means that very detailed topographical surveys are required to predict correctly the flood extension, depth, and velocity. This aspect also suggests that different small-scale features (such as sewers, drainage systems, etc.), not considered in this study, are likely to produce significant effects in urban areas flooding scenarios.

A simplified approach, here called STREETS_GRID, can be adopted. The set-up of a "streets grid" model is relatively simple. Results are similar to those provided by the models that resolve the entire domain, at least along the streets. This model can globally simulate the effect on flood propagation due to the presence of an urban area. This conclusions hold in the case of steady flow, for which the presence of storage areas (e.g. gardens and other green areas) makes no effect. In the case of time varying condition, reported in paragraph 2.3, storage areas nearby the streets are likely to produce larger flooded areas and, as a consequence, to reduce water depth and flow velocity along the streets. On the contrary, simplified models that consider only the street produce larger water depth and flow velocity, resulting in a faster propagation through the urban area.

Modelling techniques that resolve the water motion in urban areas with extremely high-resolution, while seeming necessary to capture all the significant processes involved in urban flooding, poses a different kind of problem. Indeed, modification of small-scale elements are relatively often, thus making difficult to maintaining the flooding model up to date. As an example, the renovation of garden walls, as well as, the creation of a new bicycle path or a sidewalk near to the streets, with traffic divider of limited height, are able to modify considerably the flooding pattern in an urban area. Consequently, high-resolution flooding analyses need high-resolution models to be continuously updated for obtain durable, reliable results and to determine correctly the potentially floodable area in the view of, e.g., assessment and management of the local emergency plans.

Provided that topographical surveys with sufficiently high-resolution are available, the question of cost still remains open, in terms of both gathering of data and model set-up. Indeed, modelling small-scale urban structures requires the use of a great number of very small computational elements, with problems of over-parameterization and execution time. Moreover, this kind of extremely deterministic approach does not face with modelling uncertainty, nor is suitable to be used in probabilistic framework (e.g., Montecarlo approaches), where multiple simulations have to be performed.

As an example, the 0.4_WALL mesh need a computational timestep that is about 0.1 times that needed by the STREETS_GRID mesh, which correspond to a 10 times greater execution time. This is due to the limited dimension of the 2D elements that described the walls. Accordingly, from a practical point of view, model with high-resolution features, due to their long computational time and complex structure, can be used only in few cases.

When considering very large areas, such as in the case of analyses at the catchment scale, the use of high-resolution turns out to be critical. As said before, this is because the mesh generation and the computational demand become very demanding tasks.

We can conclude that flooding simulation in urban areas is a very challenging task. In the case of poor availability of data, the model could not capture significant or even critical processes; on the other side, too many available data are difficult to be managed, and yield to high-resolution, burdensome models, not applicable to large-scale analyses.

3 Subgrid modelling in urban areas

The challenge addressed in this chapter is how to extend a process-based model, which accounts for building high-resolution geometry, to the catchment scale.

The fundamental issue is that the mesh elements at catchment scale, due to computational limits, can only resolve features larger than the small-scale structural elements used for a building-scale analysis. Consequently, subgrid models are used in order to consider topographic variability that are too small to be explicitly simulated but are important for the macroscopic representation of flood events.

3.1 Introduction

Different approaches are tested and analyzed for subgrid modelling. Two of these methods have been already used in the 2DEF model for similar purpose. The third model is a new approach created specifically for solve topographic variability in urban areas.

In the first subgrid model, a special element globally simulates the effects of the presence of buildings, and needs three parameters: the buildings density inside the urban area (used in the continuity equation), the effective buildings density due to structures shielding effects (used in dynamic equation), and a correction of mean length paths. From a theoretically point of view, this special element is descripted in some details in the Appendix C as "urban area special element". This method does not consider the possible formation of preferential pathways in different directions and, for this reason, is regarded as an isotropic approach.

The second method applies to the computational elements, included in an urban area, different values of bottom friction parameters for the two main directions. This method was initially developed for rural areas in order to simulate the regular presence of ditches and furrows. These modified bottom friction parameters are assumed to simulate, by decreasing or increasing the Gauckler-Strickler parameters, the anisotropic global resistance produced by the regular disposition of buildings and the creation of preferential pathways. The values for the new bottom friction parameters are hard to be gathered by a pure physically based approach. Accordingly, the Gauckler-Strickler parameters, needs to be calibrated in order to obtain reliable results.

A third approach is created and applied for the first time within the 2DEF model. It moves from the need of using physically based subgrid modelling that includes the global resistance of buildings and the formation of preferential pathways. This method is based on the evaluation of an artificial porosity. The artificial porosity used in this approach is defined as the ratio of the cross-sectional area available to the flowing of water and the total cross-sectional area. This artificial porosity represents the reduction of cross-sectional area due to the presence of buildings and, consequently, it estimates the global resistance of the urban area. This artificial porosity is set for the two principal directions, the mutual difference representing the magnitude in terms of anisotropy, due to the presence of preferential pathways.

3.2 Approach A: special isotropic elements

All the computational elements included in the urban area are set as special elements. Flow preferential pathways cannot be considered in these special elements so this method turns out to be an isotropic approach. The magnitude of streets rotation, the position of houses, walls and the structures shape have no effect in subgrid simulation with approach A. As briefly described in the introduction of the Chapter 3 and, in more details, in Appendix C, the only physically based parameter to be included in these special elements is the ratio of the area occupied by structures to the total urban area (buildings density). Starting from this consideration, it is possible to compare this approach only with the high-resolution models NO_WALL and STREETS_GRID used in Chapter 2. Analogies with model that consider the presence of walls, as high-resolution models 0.2_WALL and 0.4_WALL, are more difficult to be carried out.

3.2.1 Urban area schematic application

In analogy with the NO_WALL model, special elements are set with buildings density, as described in the Appendix C. The buildings density results equal to 0.22 for the considered urban area and is calculated directly using topographical data (Figure 3.1).

In the following figure the area occupied by buildings (yellow) and the free area (light blue) are identified.

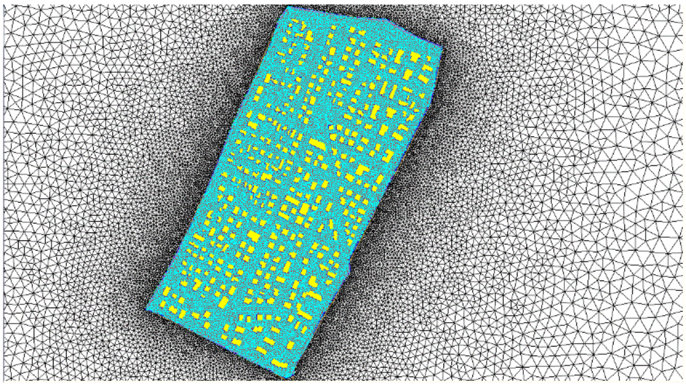

Figure 3.1 Schematic calculation for buildings density (NO_WALL analogy)

Other parameters are the effective density, set equal to the buildings density, and the parameter expressing the mean lengthening of paths, set equal to unity. Model parameters used for the simulation are the same adopted in the second chapter.

The results for special elements approach and for NO_WALL model are reported below (Figure 3.2 and Figure 3.3). The area described with special elements is partially covered in order to highlight the effect of subgrid modelling in the external area.

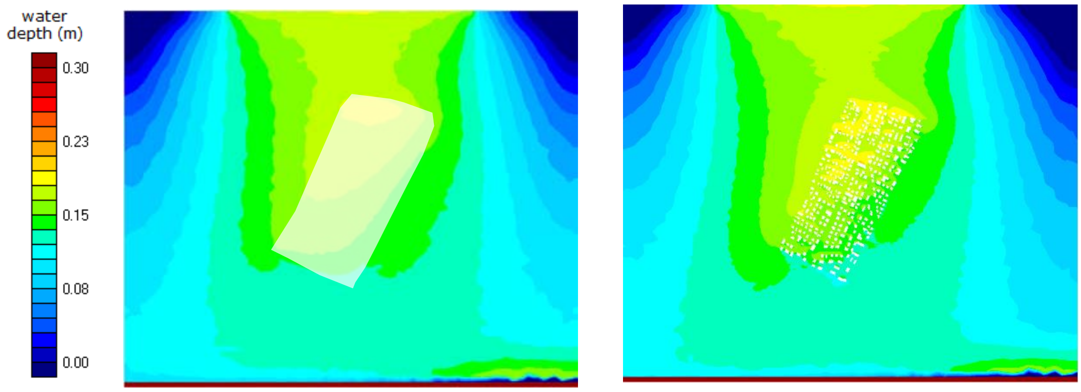

Figure 3.2 "Urban area" special elements vs. NO_WALL model (water depth distribution)

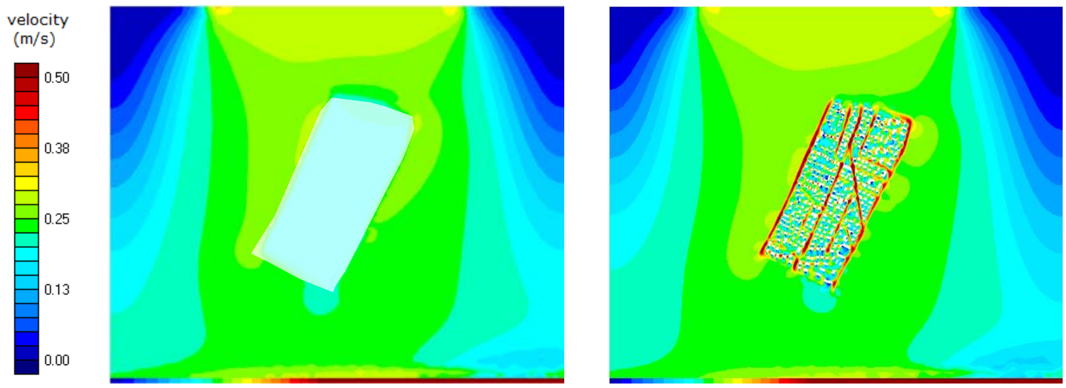

Figure 3.3 "Urban area" special elemets vs. NO_WALL model (velocity distribution)

Analyzing the previous images is possible to notice that, in this case, the application of special elements is able to simulate the global resistance effect of the urban area. Special elements are not able to simulate the anisotropic behavior of the flow, which deviate the flow towards the left side (Figure 3.2).

In analogy with the STREETS_GRID model, special elements are set with the ratio of the area occupied by houses and garden to the total area. This parameter is insert in the special elements characteristic as described in the Appendix C. In this case, the structures density results equal to 0.78, and is calculated geometrically (Figure 3.4). The following figure identify the area occupied by buildings and gardens (in yellow) and the free area (light blue).

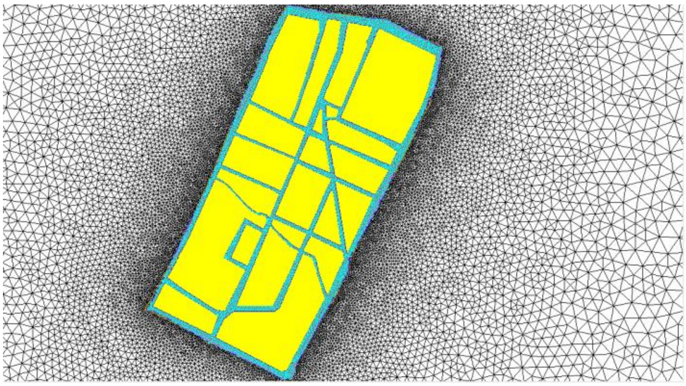

Figure 3.4 Schematic calculation for structures density (STREETS_GRID analogy)

Other parameters are taken in analogy with the previous case.

The results of this approach and of the STREETS_GRID model are reported below.

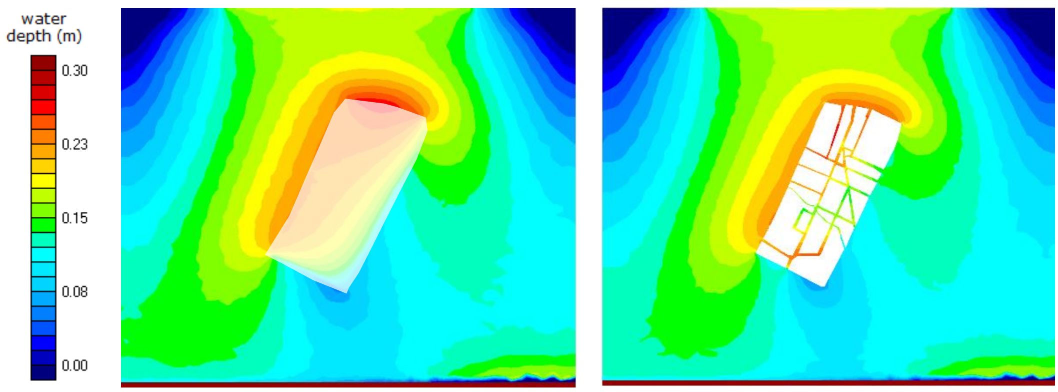

Figure 3.5 "urban area" special elements vs. STREETS_GRID model (water depth distribution)

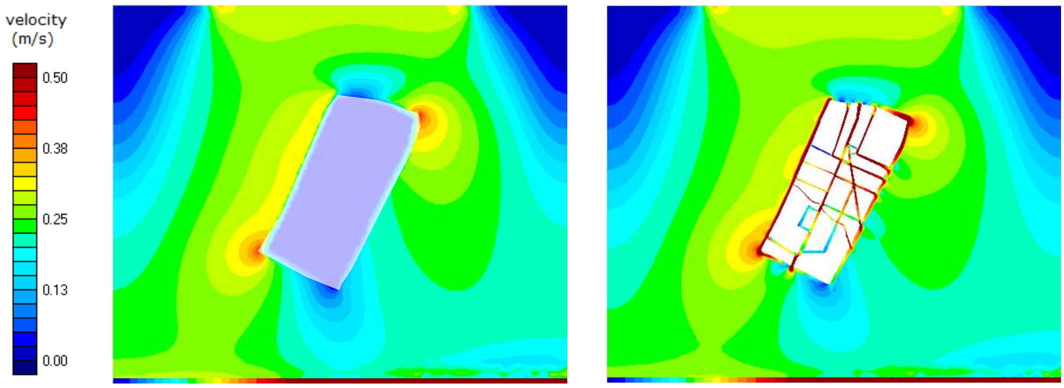

Figure 3.6 "urban area" special elemets vs. STREETS_GRID model (velocity field distribution)

In this case, the simulation with special elements seems to be more effective. The global resistance of the urban area is lightly overestimated in the upper part of the urban area (red area in Figure 3.5) and remain some errors in water depth distribution due to the lack of anisotropic capabilities of these special elements.

3.2.2 Approach A discussion

The subgrid model representing the urban area as series of special, isotropic elements, from the analysis reported previously, seems to be effective, although with some limitations.

The applications of approach A models are useful only if the simulated urban area is sufficiently homogeneous and isotropic. This partial efficiency is connect to the assumption underlying the definition of these special elements. The fundamental parameter is the ratio of the area available for water flow to the total area.

Therefore, this technique simulates efficiently the global resistance of the urban area due to the reduction of floodable area (equation (C.3) in Appendix C). On the contrary, no information are included that regards the position and the shape of buildings inside the urban area: consequently, the presence of possible preferential pathways could not be simulated. This fundamental parameter is anyway very simple to be calculated a priori from geometrical information so, in suitable urban areas, this method give reliable results with a good predictive ability.

Some problems, on the contrary, are associated to the evaluation of the other parameter, which can be set in this type of special elements. The reduction of area that affects the dynamic, in addition to the storage capacity, even if physically based, is more difficult to be evaluated. The same consideration could be done for the parameter that represents the lengthening of paths to buildings presence. These two parameters, due to their difficult a priori evaluation, need to be calibrated or assumed based on the modeler experience, thus reducing the predictive ability of this approach.

The limits shown by an isotropic approach suggest the use of a model that consider the anisotropic characteristic of urban areas.

3.3 Approach B: anisotropic bed shear stress

This approach was initially developed to simulate the resistance that water flow experiences in different directions due to the presence of particular, anisotropic structures. This model was applied, in particular, to rural areas where furrow and ditches, built for drainage purpose, highly modify the flow directions from that of the maximum slope. The assumptions of anisotropic behavior used in the development of this model are analyzed and the possibility of correctly applying it in urban area applications is considered.

3.3.1 Model description

The solution of De Saint Venant's equations with bed shear stress anisotropy hypothesis is reported below. The continuity equation is not considered because bed shear stress only affects the dynamic equation.
Defining the different bed shear stress under anisotropic conditions, an orthonormal system of axes is selected that correspond to the direction of minimum and maximum bottom resistance (other hydraulic condition being equal). The axes are called "Longitudinal" for minimum resistance direction and "Transversal" for maximum resistance direction. Considering Gauckler and Strickler parameter (the same used in the model) the equivalent condition is that the "Longitudinal" Gauckler and Strickler parameter is higher than the "Transversal" one, so $k_{SL}>k_{ST}$. The following condition holds for bed shear stresses $\tau_L<\tau_T$. This system of orthonormal axes, hereafter defined as L-T axes, is rotated of an arbitrary α angle compared to the x-y system used for solving the model equations (Figure 3.7).

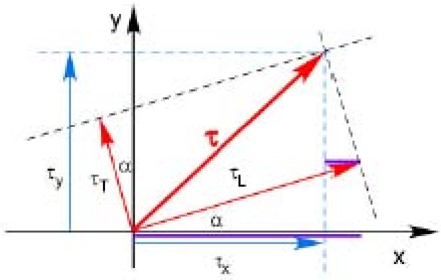

Figure 3.7 Orthonormal axes definition

In the De Saint Venant equations (equations (A.1) and (A.2) in the Appendix A), shear stress component along x-y frame could be replaced with component along L-T axes using this geometrical relationship, derived from Figure 3.7:

$$\begin{cases} \tau_x = \tau_L \, cos\alpha - \tau_T \, sin\alpha \\ \tau_y = \tau_L \, sin\alpha + \tau_T \, cos\alpha \end{cases} \tag{3.1}$$

Starting from the fundamentals equations described in the Appendix A, the general equation for bed shear stresses reads:

$$\tau = \gamma \, Y \, j \tag{3.2}$$

Where the τ is the bed shear stress, γ is the water specific weight, Y represents the volume of water for a generic surface area and j is the linear hydraulic head loss.

Following the Gauckler Strickler formulation is possible to define the velocity:

$$v = k_s \, R_H^{2/3} \sqrt{j} \tag{3.3}$$

The hydraulic radius R_h is defined as the ratio of the cross-sectional area to the wetted perimeter.

For shallow water is possible to calculate the hydraulic radius considering that the width of the cross-sectional area, b, is much larger than the water depth Y.

$$R_H = \lim_{\left\{\frac{b}{Y}\to\infty\right.} \frac{b\,Y}{2Y+b} = Y \tag{3.4}$$

From equation (3.4) is possible to define R_H=Y. Substituting this result in the Gauckler Strickler equation (3.3) and adjusting it is possible to obtain:

$$j = \frac{v^2}{k_S^2\ Y^{\frac{4}{3}}} \tag{3.5}$$

Merging the equations (3.2) and (3.5):

$$\tau = \gamma\, Y\, j = \frac{\gamma\, Y\, v^2}{k_S^2\ Y^{\frac{4}{3}}} \tag{3.6}$$

Considering the L-T axes, we have:

$$\begin{cases} \tau_L = \dfrac{\gamma\, Y\, v_L\, |v|}{k_{SL}^2\ Y^{\frac{4}{3}}} \\[2ex] \tau_T = \dfrac{\gamma\, Y\, v_T\, |v|}{k_{ST}^2\ Y^{\frac{4}{3}}} \end{cases} \tag{3.7}$$

The equations reported in (3.7), which represent the definition of bed shear stress along the L-T axes, are applied in the model by means of (3.1).

3.3.2 On the existence of isotropic, equivalent roughness coefficient

We may ask if, in the case of anisotropic bed roughness, it makes sense to estimate an isotropic, equivalent roughness coefficient.
This equivalent parameter is calculated starting from the expression of longitudinal and transversal, anisotropic components.

Starting from the Figure 3.7, bed shear stresses along the L-T axis are compared with equivalent bed shear stresses.

$$\tau_{eq} = \sqrt{\tau_L^2 + \tau_T^2} \tag{3.8}$$

Applying to the previous equations (3.8) the equations for the bed shear stresses (3.7) and (3.6) is possible to obtain the general equation:

$$\frac{\gamma\, Y\, v\, |v|}{k_{Seq}^2\;\, Y^{\frac{4}{3}}} = \frac{\gamma\, Y\, |v|}{Y^{\frac{4}{3}}} \sqrt{\frac{v_L^2}{k_{SL}^4} + \frac{v_T^2}{k_{ST}^4}} \tag{3.9}$$

Simplifying the equation (3.9), we obtain:

$$\frac{v}{k_{Seq}^2} = \sqrt{\frac{v_L^2}{k_{SL}^4} + \frac{v_T^2}{k_{ST}^4}} \tag{3.10}$$

Dividing by v, we have:

$$\frac{1}{k_{Seq}^2} = \sqrt{\frac{\left(\frac{v_L}{v}\right)^2}{k_{SL}^4} + \frac{\left(\frac{v_T}{v}\right)^2}{k_{ST}^4}} \tag{3.11}$$

We define β as the angle formed by flow velocity compared to the L axis. We have:

$$v_L = v * \cos\beta \;\rightarrow\; \frac{v_L}{v} = \cos\beta$$
$$v_T = v * \sin\beta \;\rightarrow\; \frac{v_T}{v} = \sin\beta \qquad (3.12)$$

Substituting equations (3.12) into (3.11), we have:

$$\frac{1}{k_{Seq}^2} = \sqrt{\frac{cos^2\beta}{k_{SL}^4} + \frac{sin^2\beta}{k_{ST}^4}} \qquad (3.13)$$

For verification purpose, on can be observe that setting k_{SL}=k_{ST}, which is equivalent to assume isotropic condition, the result is k_{SL}=k_{ST}=k_{Seq}

Analyzing Eq.(3.13), we observe that the equivalent bed shear stress depends not only from roughness parameters in longitudinal and transversal direction, but also from the direction of the flow, defined from the angle β.

This is an important conclusion as it shows that the equivalent bed shear stress is dependent on flow direction. Since the velocity direction is not a priori known, we can conclude that it is not possible to reproduce the anisotropic effect by applying an equivalent isotropic roughness value. If angle β, representing the variation in direction of flow velocity compared to L axis, changes, also the equivalent roughness parameters changes.

The Figure 3.8 describes the variation of the equivalent roughness parameter as a function of β, as defined by Eq. (3.13).

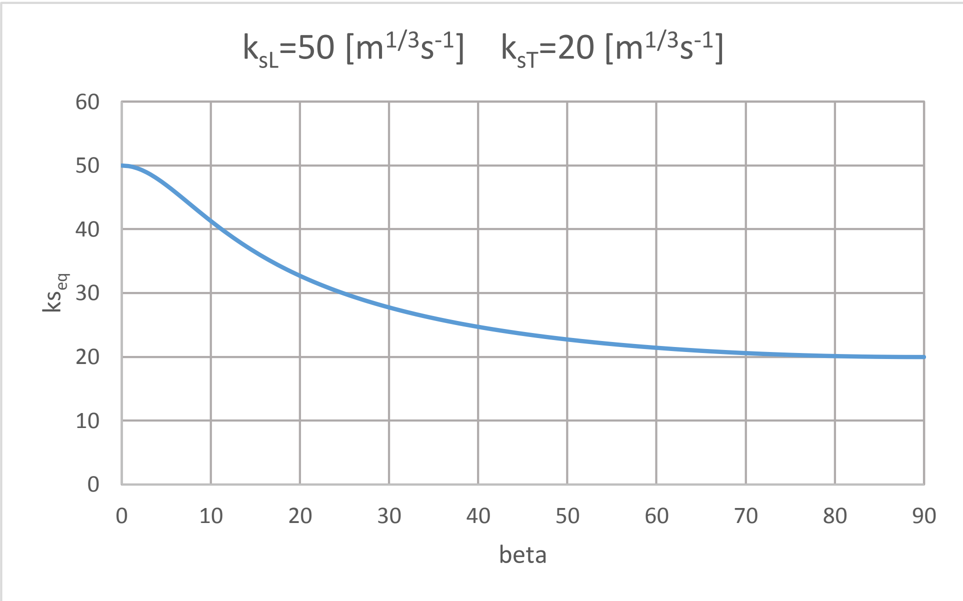

Figure 3.8 Equivalent bed shear stress values compared to angle β

3.3.3 Approach B discussion

As deduced from the application of the approach A subgrid model, the simulation of anisotropic effects in urban areas is fundamental in some cases. In Approach B, the anisotropic behavior is considered by assuming different values of the Gauckler Strickler parameter along orthogonal, principal directions. In Section 3.3.2 we demonstrated that a reduction of anisotropic characteristic to an equivalent, isotropic model is not feasible, i.e., we cannot define an equivalent isotropic roughness parameter starting from the two anisotropic values, since the magnitude and the direction of stress strongly depend on the direction of flow with respect to the principal frame.

On the other hand, the anisotropic characteristics of an urbanized area originates from the blockage effect of buildings, i.e., the major macroscopic resistances are shape resistance rather than wall resistance. This means that the tuning of the Gauckler Strickler parameters in the model, to account for building anisotropy effects, is merely a conceptualization of these parameters. This loss of physical meaning leads to the need of calibrating the k_s parameter to match specific result, but no warranty is offered about the model behavior out of the calibration field. The predictive skills of the Approach B are expectably low: for this reason, model application using this approach have not been reported in the thesis.

3.4 Approach C: a new anisotropic artificial porosity model

In the scientific literature, subgrid scale parameters that correspond to void ratios have been codified as "artificial porosity" and urban flood models that utilize porosity have shown promising results relative to the challenge of extending process-based urban flood models to the catchment scale (Yu and Lane 2006, Sanders 2008, Guinot 2012). The most common definition of porosity, in a volumetric sense, is the fraction of a control volume occupied by voids. Another definition of porosity is obtained by considering a slice through a porous medium. The fraction of the cross-sectional plane occupied by voids represents an areal porosity.

Distinction between volumetric and areal porosity is appealing and potentially important because areal porosity is an anisotropic characteristic, which offers the possibility of resolving preferential flow directions and the alignment of buildings along streets (e.g., Sanders 2008). This artificial porosity, defined for different direction, is suitable to simulate the urban area anisotropy.

Different model conceptualization with areal porosity was applied in literature. In this thesis, a completely new theoretical approach is developed and applied to the 2DEF model.

3.4.1 Description of the "artificial porosity" model

In this thesis, for the first time, a new version of 2DEF model is used and tested. In this version, the bottom friction parameter is not considered as the principal source of anisotropy. A new parameter is here introduced, which refers to the concept of artificial porosity.

The artificial porosity defines, in a high-resolution analysis and for a given direction, the ratio of the cross-sectional area available for water flowing to the total cross-sectional area. This parameter is defined, for analogy, as an areal porosity. Actually, when considering high buildings this artificial porosity becomes a sort of length ratio.

An example is reported in Figure 3.9 for the calculation of the artificial porosity in a schematic case.

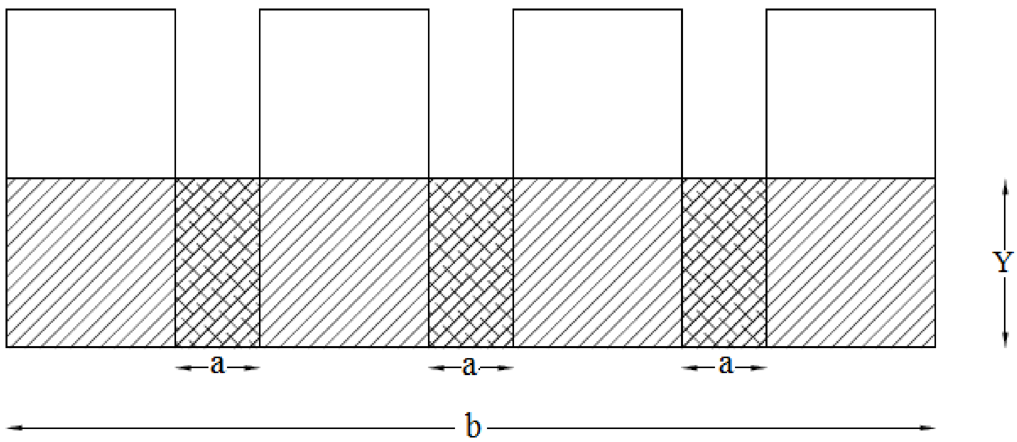

Figure 3.9 Cross-sectional view for definition and the calculation of artificial areal porosity

Using the simple example in Figure 3.10 is possible to explain theoretically the approach C to urban modelling.

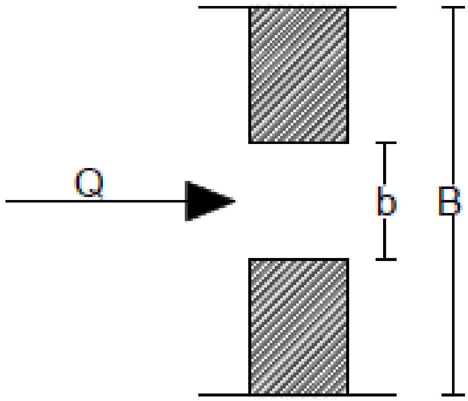

Figure 3.10 Planar view for the theoretical explanation of approach C model

Looking at Figure 3.10, we can write the total discharge, Q, as the product of a specific flow rate (i.e., the depth-integrated velocity) and a reference width:

$$Q = q' \, b = q \, B \tag{3.14}$$

We define the artificial porosity as:

$$\Psi = \frac{b}{B} \tag{3.15}$$

Merging the Eq.(3.14) and (3.15) reads:

$$q' = \frac{q}{\Psi} \tag{3.16}$$

The Eq. (3.16) converts the specific flow rate in the presence of obstacles that partially fill the cross sectional area.

Considering the presence of the obstacles, and accounting for the actual depth integrated velocities, we have (equation (A.9) in the appendix A for theoretical explanation):

$$\frac{\tau}{\gamma\, Y} = \frac{|q'|\, q'}{k_S^2\, Y^{\frac{10}{3}}} \tag{3.17}$$

By using Eq. (3.16), we obtain the shear stress in terms of macroscopic variables q and Y.

$$\frac{\tau}{\gamma\, Y} = \frac{|q|\, q}{k_S^2\, \Psi^2\, Y^{\frac{10}{3}}} \tag{3.18}$$

Finally, for the longitudinal and transversal axis the shear stress components are:

$$\begin{aligned} \frac{\tau_L}{\gamma\, Y} &= \frac{|q|\, q_L}{(k_{SL}\, \Psi_L)^2\, Y^{\frac{10}{3}}} \\ \frac{\tau_T}{\gamma\, Y} &= \frac{|q|\, q_T}{(k_{ST}\, \Psi_T)^2\, Y^{\frac{10}{3}}} \end{aligned} \tag{3.19}$$

We can now use Eq. (3.1) to project the shear stresses, defined in equations (3.19), from L-T frame to the x-y frame and apply this formulation to the 2DEF model.

To do this, we must specify the angle α (Figure 3.7) that define the rotation between the L-T axes and the x-y axes. These equations, implemented in the 2DEF model, define the "Approach C" modelling tool.

3.4.2 Preliminary tests

As reported before, in this thesis the approach C is applied for the first time in the 2DEF model. Before starting the simulation of urban areas flooding, preliminary test to verify the model accuracy and correctness are needed.

- Diffusion of a flood wave under severe anisotropic conditions

Consider the rectangular domain in the following Figure 3.11. The rotation angle α has been set to 45°, and the artificial porosity of all the computational elements is set equal to one and to zero (i.e., 1.E-8) for the longitudinal and the transversal direction, respectively. This means that, in the modeler intention, only L direction is available for water flow. The bottom slope is oriented from top to bottom. A discharge of 1 m^3/s enters the domain in a precise location along the upper edge of the mesh. A channel, which is positioned at the lower edge of the mesh, collects the water.

The results, in terms of water depth and velocity distribution are reported below.

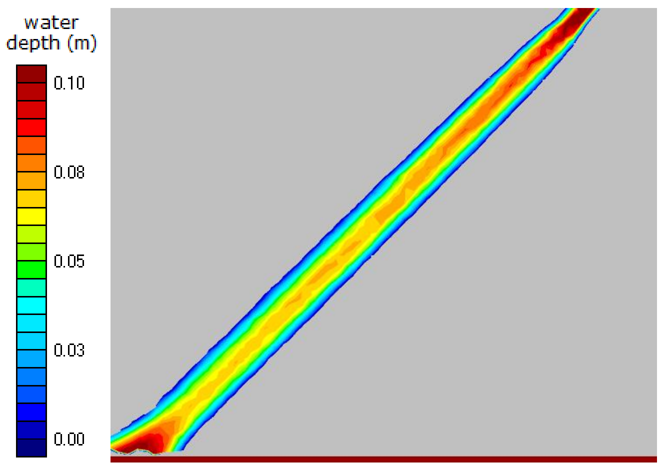

Figure 3.11 Diffusion of a flood wave on severe anisotropic set-up (water depth distribution)

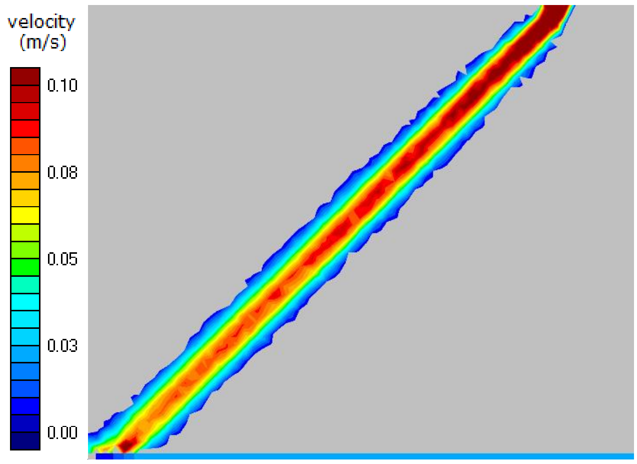

Figure 3.12 Diffusion of a flood wave on severe anisotropic set-up (velocity distribution)

As clearly shown by the previous images, this new model is able to redirect the water flux along the L direction and, at the same time, to limit the diffusion of inundation along the T direction, where flow is inhibited (i.e., $\Psi_T = 0$).

- Blockage effect

Another effect initially investigated is the ability of the model to reproduce the “blockage effect”. Along a row of computational elements we imposed $\Psi_L = \Psi_T = 0$, i.e., the artificial porosity is set equal to zero in both directions. This means that, in the modeler intention, no water could overpass this row. The computational mesh is very similar to the one used in the previous experiment The discharge enters uniformly from the central part of the upper edge of the mesh and is collected by a channel located in the lower part.

The results, in terms of water depth and velocity distribution, are reported below.

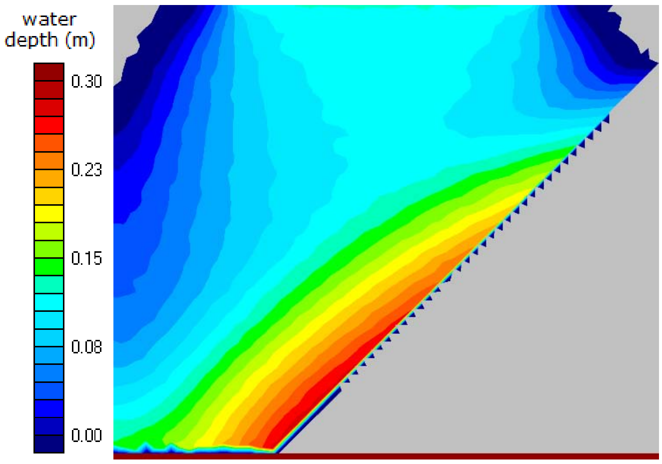

Figure 3.13 Blockage effect (water depth distribution)

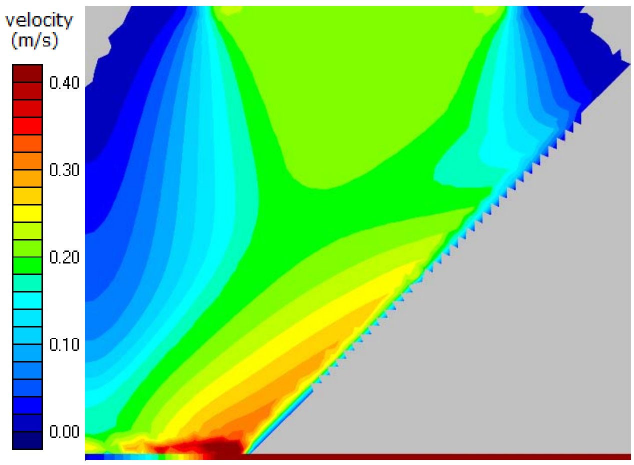

Figure 3.14 Blockage effect (velocity distribution)

From the results reported, we can conclude that the proposed subgrid approach is able to block completely the water flow when the artificial porosity is set to zero.

3.4.3 Urban area schematic application

As for the approach A in the Section 3.2, the suitability of the Approach C is here verified, in analogy with the results obtained in the second chapter.
The artificial porosity approach C is here applied in order to reproduce NO_WALL and STREETS_GRID models used in Chapter 2.

Analogies with models that consider the presence of walls, as high-resolution models 0.2_WALL and 0.4_WALL, are harder to be found, because in such cases we cannot assume that the areal porosity is constant with the water depth.

- NO_WALL model

In analogy with NO_WALL model, the artificial porosity is calculated in the longitudinal and transversal directions as described in Section 3.4.1. In this case, only the areas occupied by houses are not available for water flowing. The artificial porosity results equal to 0.40 along the longitudinal direction and 0.35 along the transversal direction. These values are calculated directly from geometrical considerations as described in Figure 3.15.

From the following figure is possible to identify the area occupied by houses (yellow) and the free flow area (light blue), along the longitudinal and the transversal direction, respectively.

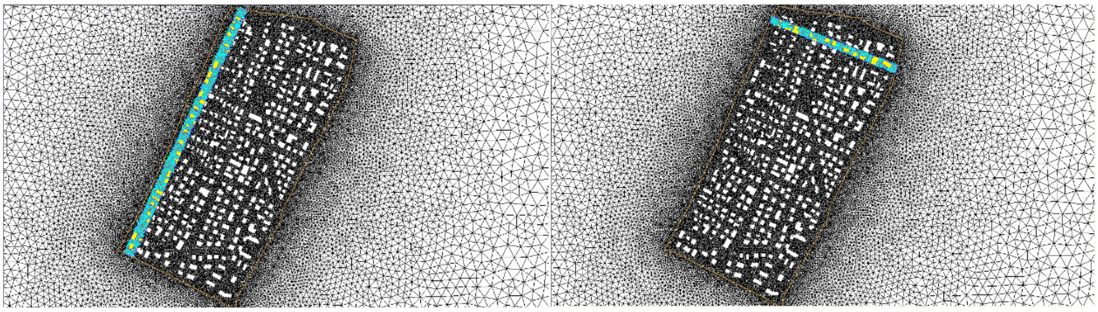

Figure 3.15 Schematic calculation for artificial porosity (STREETS_GRID analogy)

The rotation angle of the L-axis with respect to x-axis is set equal to 65°. Other model parameters are the same adopted in the second chapter. The results of the model with artificial porosity and NO_WALL model are reported together for comparison purpose.

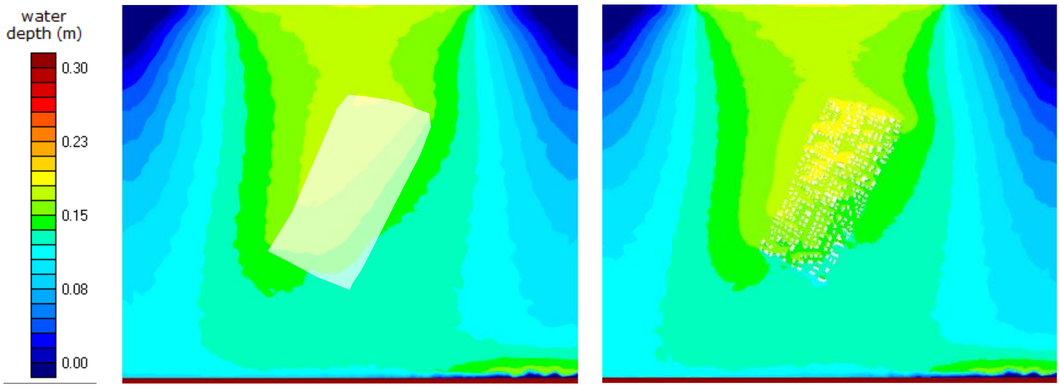

Figure 3.16: Water depth distribution obtained using artificial porosity approach (left) and NO_WALL model (right)

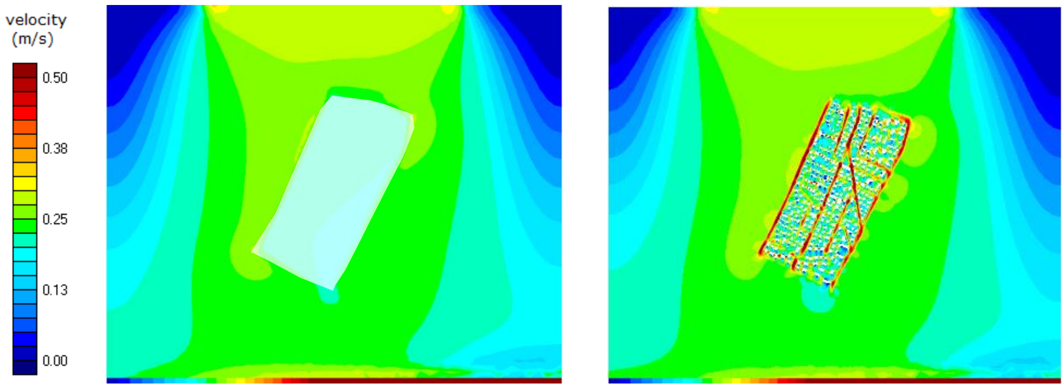

Figure 3.17 Velocity distribution obtained using artificial porosity approach (left) and NO_WALL model (right)

From a macroscopic point of view (i.e., just out the urbanized area) the previous images clearly show the very good agreement between the two different approaches. As expected, the areal porosity approach is able to simulate the global resistance and the asymmetry of the flow, which blend toward the left side (see also the comparison with the Figure 3.2 and Figure 3.3 where anisotropy is not accounted for).

- STREETS_GRID MODEL

For comparison purpose with the STREETS_GRID model, the artificial porosity is calculated in longitudinal and transversal directions as described in Section 3.4.1. In this case, both the areas occupied by houses and gardens are not available for water flowing. The artificial porosity results equal to 0.14 for longitudinal direction and 0.08 for transversal direction.

The anisotropic effect is here relatively stronger. The following figures identify the area occupied by houses and gardens (yellow) and by the streets (light blue).

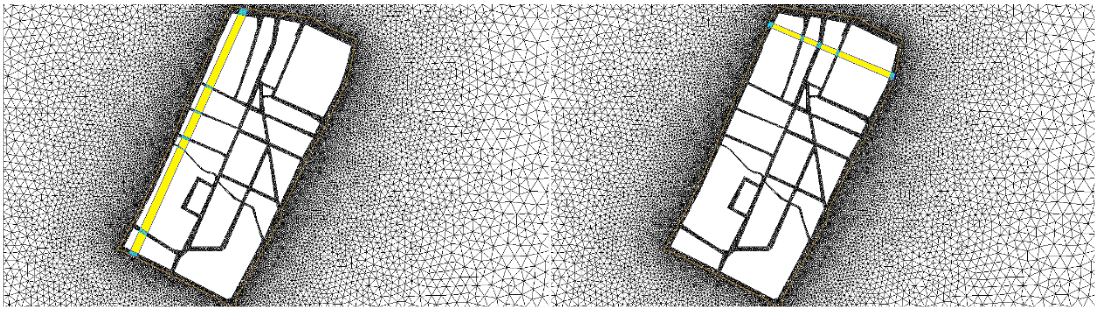

Figure 3.18 Schematic calculation for artificial porosity (STREETS_GRID analogy)

As in the previous case, the rotation angle of the L-axis with respect to the x-axis is set equal to 65°. Other model parameters, used in the simulation, are the same adopted in the second chapter. The results of the model with artificial porosity and the STREETS_GRID model are reported together for comparison purpose.

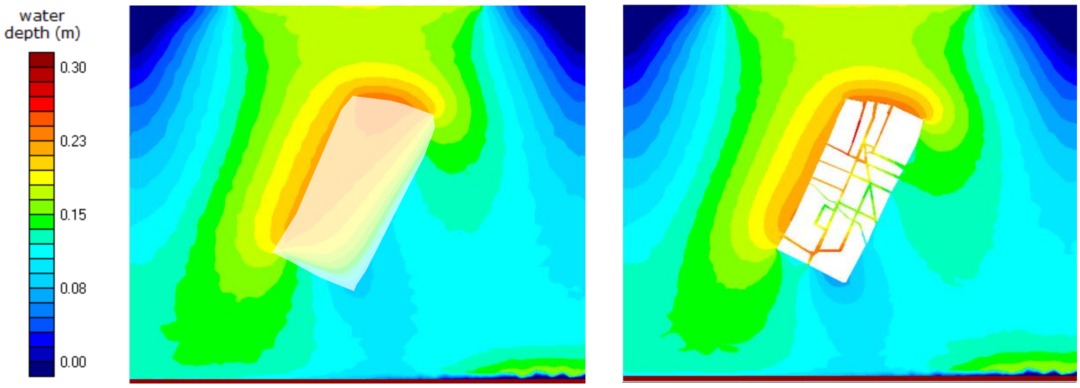

Figure 3.19 Water depth distribution obtained using artificial porosity approach (left) and the STREETS_GRID model (right)

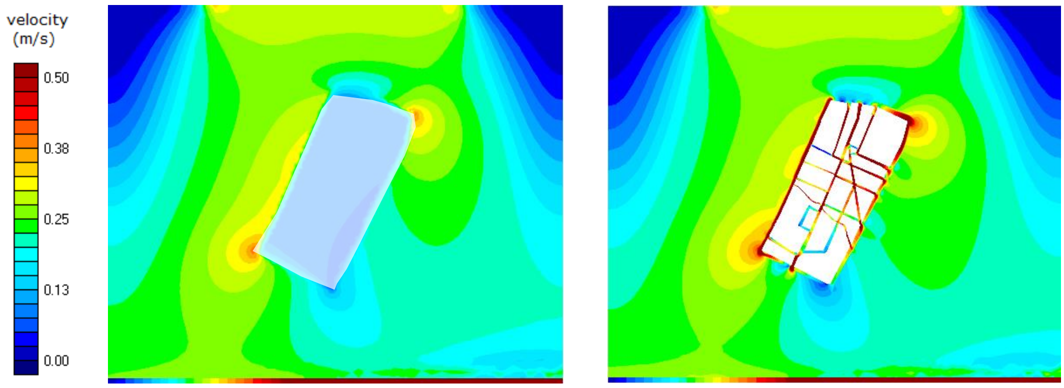

Figure 3.20 Velocity distribution obtained using artificial porosity approach (left) and the STREETS_GRID model (right)

These images clearly show an optimal agreement from a macroscopic point of view. As expected, the artificial porosity is able to simulate the global resistance and is able to simulate correctly the asymmetry of the flow, which blends toward the left side (compare also with the Figure 3.5 and Figure 3.6).

3.4.4 A further example with more pronounced anisotropy

An additional comparison is carried out simulating a simple geometrical configuration for better explain the potentially of the artificial porosity approach and for furtherly test the characteristic of this model approach compared to the application of the subgrid, isotropic model with special elements (Approach A).
The considered geometrical configurations shows a strong anisotropy and clear geometrical characteristics.

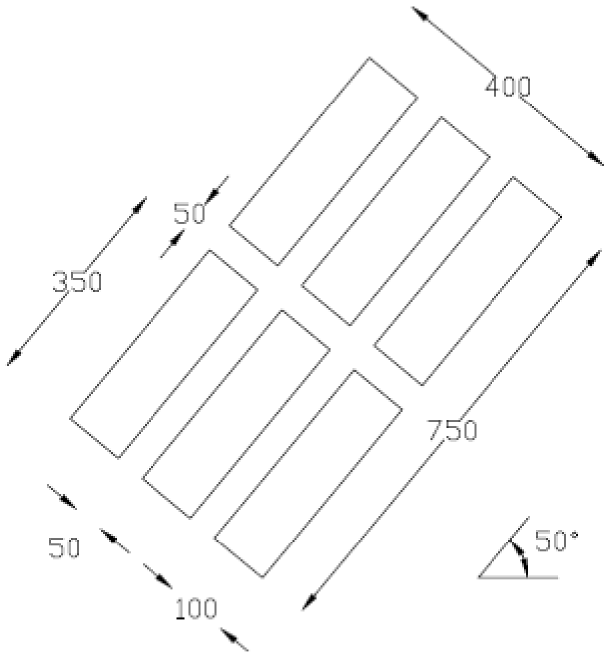

Figure 3.21 Schematic geometrical representation of a simple well-organized urban area

From the simple geometry described in Figure 3.21 is possible to calculate the artificial porosity along the longitudinal and the transversal directions.

Along the longitudinal direction, two spaces of 50 m are available to water flowing in a total width of 400 m. By applying the definition of artificial porosity explained in Section 3.4.1 we have:

$$\Psi_L = \frac{50 + 50}{400} = 0.250$$

In the transversal direction, a space of 50 m is free to water flow in a total width of 750 m. Applying the definition in Section 3.4.1 we have:

$$\Psi_T = \frac{50}{750} = 0.067$$

The rotation angle of the L-T frame with respect to the x-y frame is, for construction, equal to 50°.

These three parameters, geometrically calculated, are sufficient for model calculation using artificial porosity.

Also for the approach A (i.e., special elements isotropic model), the geometrical information from Figure 3.21 can be used to determine the fundamental parameter, i.e., the buildings density:

$$\frac{A_{Free}}{A_{TOT}} = 1 - \frac{A_{Structures}}{A_{TOT}} = 1 - \frac{(100 * 350) * 6}{(750 * 400)} = 0.300$$

This parameter, geometrically calculated, is sufficient for model calculation with the approach A. Other parameters are assumed as in the previous cases.

In conclusion, it is possible to simulate the area described in the Figure 3.21 using three different models. The first one is obtain describing directly the structures inside the model as in a high-resolution analysis. The second one is obtained using artificial, anisotropic porosity in the longitudinal and transversal directions. The last one is obtained applying the isotropic special elements "urban area" with the buildings density. The results are reported in the Figure 3.22 for comparison purpose.

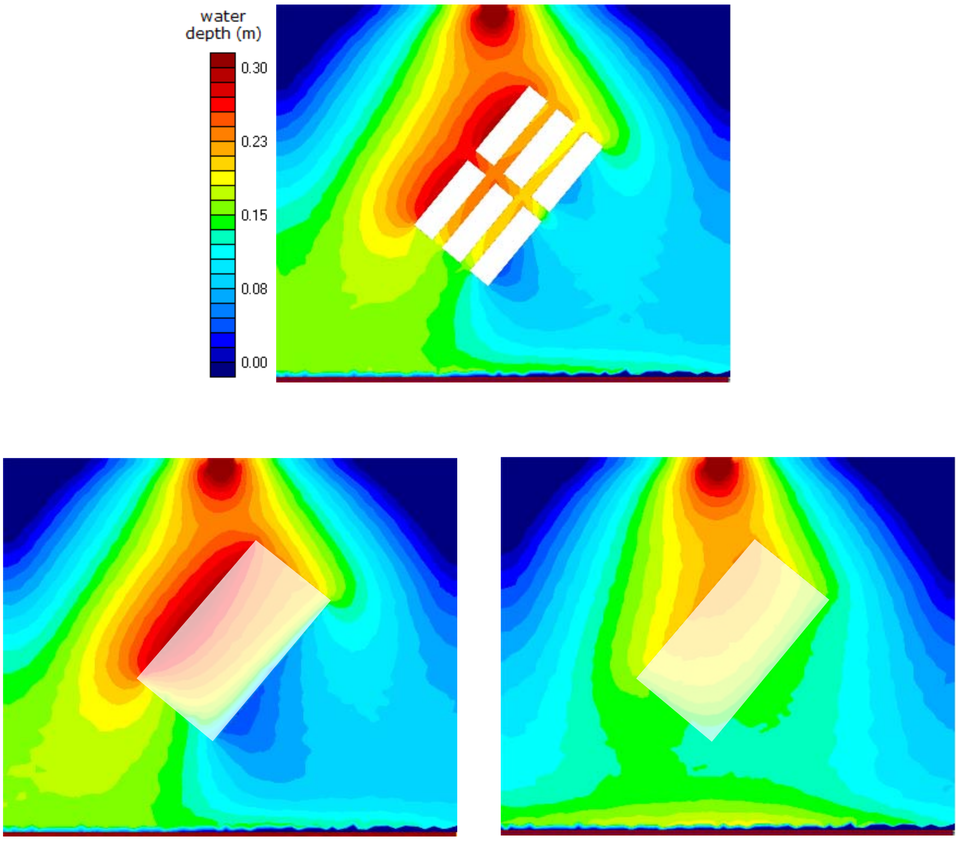

Figure 3.22 Water depth distribution obtained using high-resolution analysis (top), artificial porosity anisotropic approach (left) and isotropic special elements approach (right)

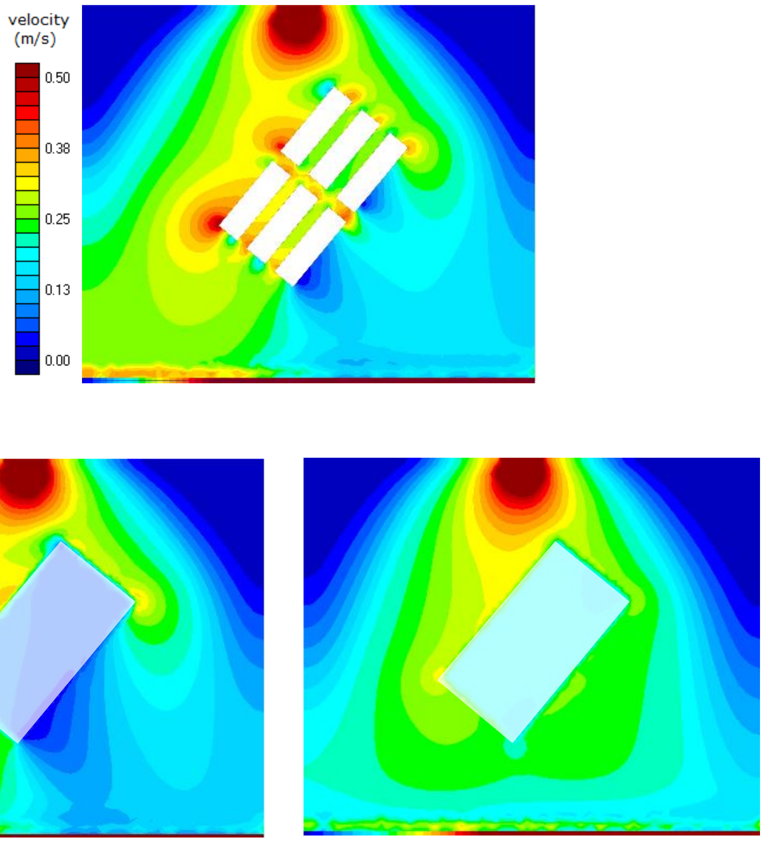

Figure 3.23 Velocity distribution obtained using high-resolution analysis (top), artificial porosity anisotropic approach (left) and isotropic special elements approach (right)

The results reported in Figure 3.22 and Figure 3.23 show that the artificial porosity anisotropic method, compared to special elements method, is largely more efficient and reliable. Starting from simple geometrical calculation, the artificial porosity method is able to fit correctly the results obtained by directly simulating the structures inside the urban area with a high-resolution mesh. Some local difference remain that are connected to the necessary simplifications required in a subgrid scale analysis.

3.4.5 Computational elements resolution

An additional test is performed for artificial porosity method, which regard the effects related to changes in the mesh resolution.

Starting from the model utilized in the chapter 3.4.3 and, in particular, from the model used to mimic the STREETS_GRID model, a similar model is created with the same geometry and parameters but with a different mesh resolution. In particular, the mean linear dimension of computational elements is reduced by a factor of 0.5.

model	n° elements	dt(s)	time simulation
STREETS_GRID	34873	2	9m 42s
Artificial porosity (finer mesh)	9090	2	2m 6s
Artificial porosity (coarser mesh)	4820	2	59s

Table 3.1 analysis of different meshes: number of computational elements, calculation timestep (dt) and total time of calculation

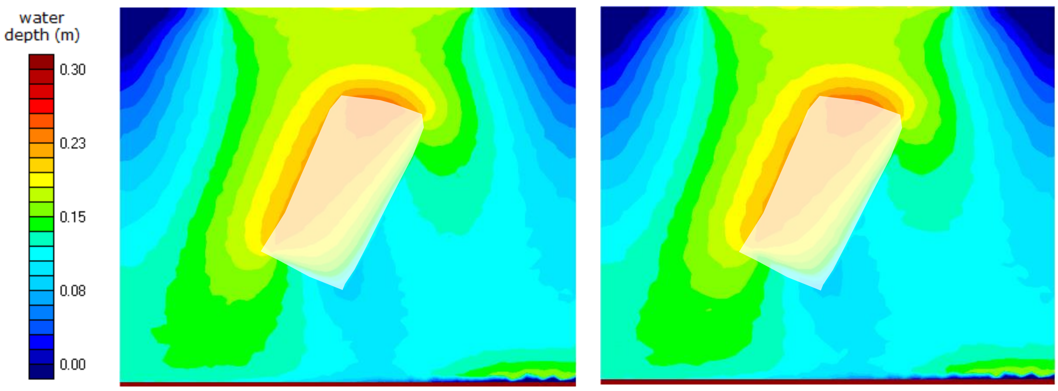

Figure 3.24 Artificial porosity approach: water depth obtained using a finer (left) and a coarser mesh (right)

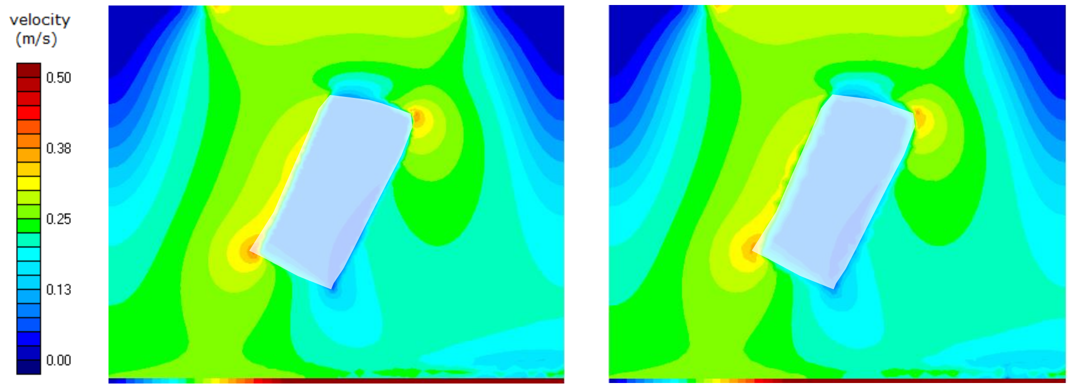

Figure 3.25 Artificial porosity approach: velocity obtained using a finer mesh (left) and coarser mesh (right)

Figure 3.24 and Figure 3.25 show that the artificial porosity method allow reducing the number of computational elements used for simulation and, consequently, to reduce the calculation time, without invalidate the previous results.

3.4.6 Comparison und time varying conditions

The last test performed for the artificial porosity method is an analysis under time varying conditions. As for the chapter 2.4, a comparison between the high-resolution simulation and the equivalent subgrid model is performed in order to highlight the reliability and the predictive ability of the artificial porosity method.

In order to evaluate the limited storage capacity inside the urban area, due to the presence of different structures (e.g. buildings), the continuity equation (C.3) used in the approach A (see the Appendix C) also apply to the approach C. In other words, an isotropic correction of storage capacity in the continuity equation, based on the concept of "void fraction", is performed in each modelling technique.

In this paragraph, the coarser mesh applied in Section 3.4.5 is used. The mesh composed by a small number of computational elements is chosen to highlight the predictive capability of the model also in the view of catchment scale applications.

As for the chapter 2.3 the inflow hydrograph is imposed locally just upstream of the urbanized area.

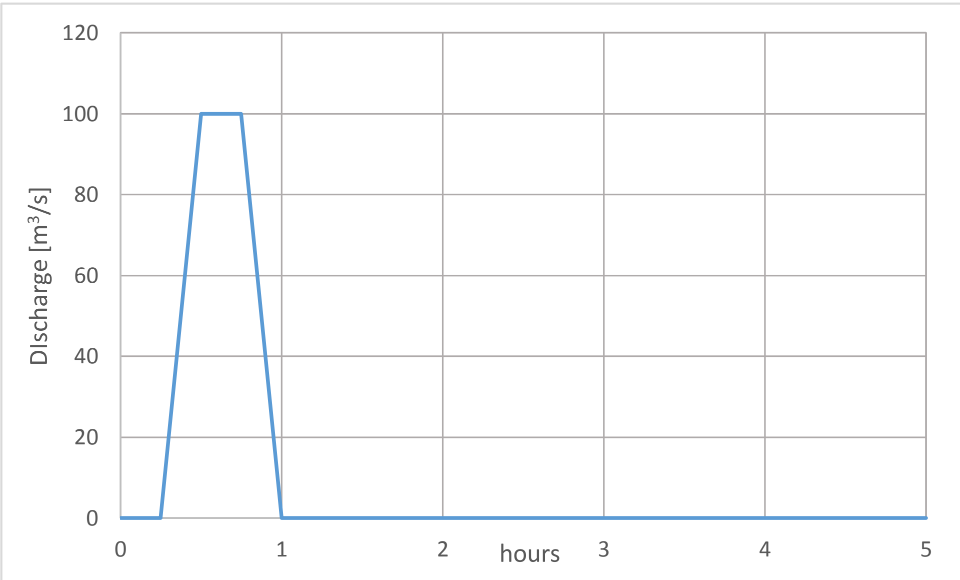

Figure 3.26 Inflow hydrograph for time varying conditions

The images reported hereafter refer to three different time instants in order to highlight the main phases of flooding.

- NO_WALL model

In order to simulate the NO_WALL model by means of the subgrid approach C, the following parameters are chosen: i) the artificial porosity is set equal to 0.40 and 0.35 for the longitudinal and the transversal direction, respectively, to account for the dynamic effects (see Section 3.4.3). ii) The buildings density is set equal to 0.22 to account for the reduced storage capacity (see Section 3.2.1).

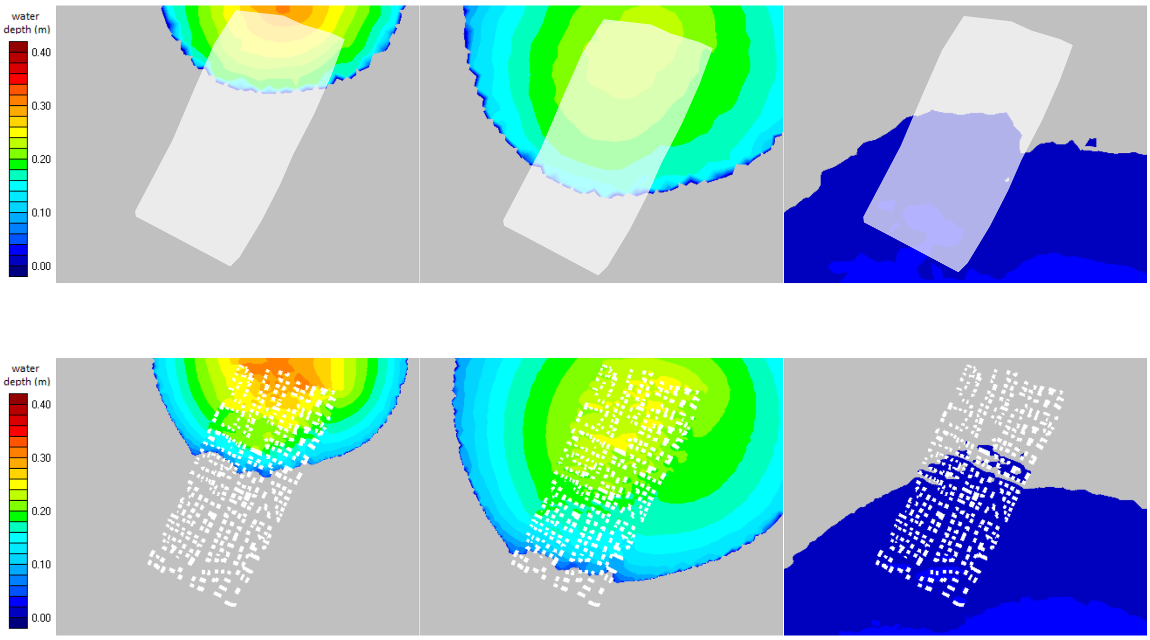

Figure 3.27 Water depth distribution of NO_WALL model (bottom) and artificial porosity model (top) for three different instants: 40 min (left), 60 min (center) and 210 min (right)

- STREETS_GRID model

In order to simulate the STREETS_GRID model by means of the subgrid approach C the following parameters are chosen: i) the artificial porosity is set equal to 0.14 and 0.08 for L and T direction, respectively, to account for the dynamic effects (see Section 3.4.3). ii) the buildings density, in which also the area of gardens are comprised, is set equal to 0.78 (see Section 3.2.1).

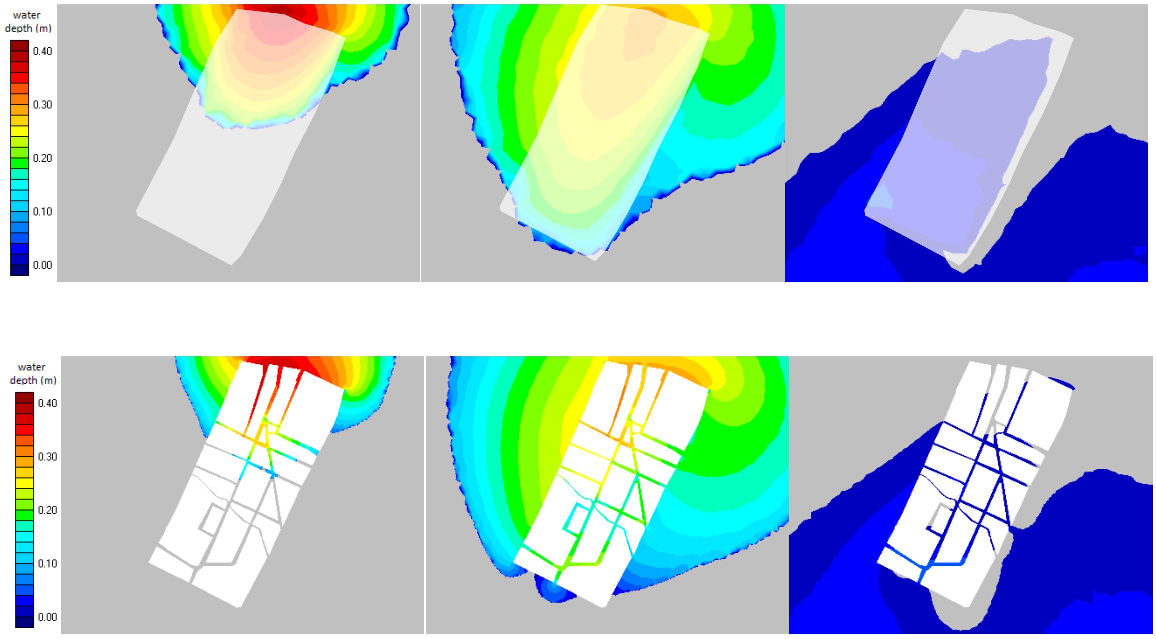

Figure 3.28 Water depth distribution of STREETS_GRID model (bottom) and artificial porosity model (top) for three different instants: 40 min (left), 60 min (center) and 210 min (right)

- 0.2_WALL model

In order to simulate 0.2_WALL model by means of the subgrid approach C, the following parameters are chosen: i) the artificial porosity is set equal to 0.14 and 0.08 for L and T directions, respectively, to account for dynamic effects (see Section 3.4.3): only the streets are considered as contributing area to water flowing (i.e., water is considered at rest in gardens). ii) the buildings density is set equal to 0.22 (see Section 3.2.1). Indeed, gardens areas, although not contributing to the water flowing, are available to water storage.

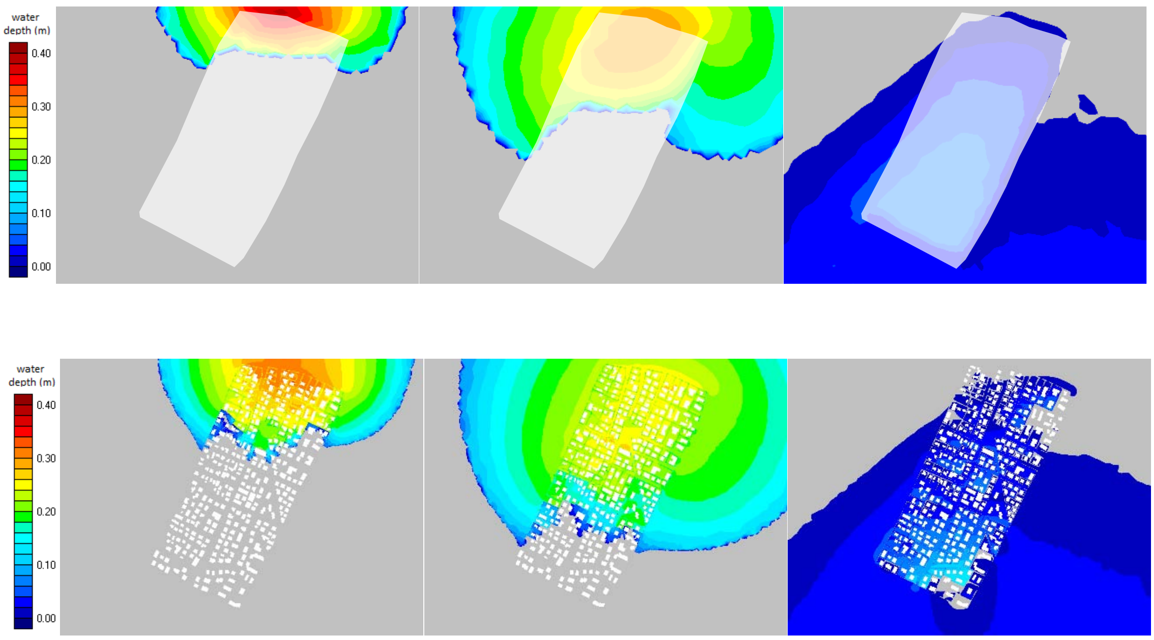

Figure 3.29 Water depth distribution of 0.2_WALL model (bottom) and artificial porosity model (top) for three different instants: 40 min (left), 60 min (center) and 210 min (right)

Figure 3.27, Figure 3.28 and Figure 3.29 show that the subgrid approach C give reliable results also for time varying condition. It is worth remarking here that all the model parameters (i.e., artificial porosity and buildings density) are a priori derived from geometrical and topographical information, and are not calibration parameters. Accordingly, the predictive skill is a key point of the proposed modelling approach. Only the comparison with the 0.2_WALL model shows a slightly lower agreement with the results of high-resolution analysis: the wave front in the subgrid model moves slower throughout the urbanized area, thus producing too many resistances. This behavior is likely because in the subgrid model the garden areas are not considered at all as contributing areas to water flowing, while, in the high-resolution model, part of water flows also through the gardens.

3.4.7 Approach C discussion

The approach C for the macroscopic modelling of urban flooding, described in the previous Sections, seems to be the most efficient and reliable method among the other here explored. This artificial porosity, anisotropic approach showed remarkable advantages over the isotropic approach already implemented in the 2DEF model to simulate the presence of urbanized areas in a large-scale, low resolution, subgrid modelling.

Compared to the special elements approach, this new approach not only is able to simulate the buildings global resistance inside the urban area, but also is able to simulate the preferential pathways that strongly modify the flow producing an anisotropic behavior.

One of the principal advantage of the artificial porosity is that model parameters are physically meaningful and can be easily inferred from geometrical, topographic data. For this reason, the predictive skill of the model is preserved, since no (or only minor) calibration is needed. In particular, compared to the anisotropic bed shear stress approach, the artificial porosity approach reduces the need of using exceptionally high and unrealistic values of the roughness parameters to represent the effects of urban structures.

The last test performed for the approach C under time-varying conditions gives an additional validation of the predictive ability of this approach.

In every simulation performed and reported in the Chapter 3, the artificial porosity approach results the most accurate and reliable method in term of good agreement with the results obtained through high-resolution simulations, but also the most efficient in terms of computational time.

4 Conclusions

This thesis focused on the analysis of urban flooding models. It was shown that modelling the flooding of urbanized areas is a challenging task for different reasons:, such as the presence of a large number of obstacles of various shapes and length scales, the storage capacity of buildings and that of partially closed areas (e.g., gardens), and the generally complex geometry and topography.

With regard to the role of small-scale features, it can be concluded that:

- little variations in the topography of urban areas can produce significant effects on flooding characteristics;
- the modelling of flooding in urban environments requires the explicit representation of small-scale topographic features in order to capture the local characteristic of flow near structural elements;
- small variations in the position and height of garden walls or gates produce non-negligible effects on flooded area extension and on the flow field, in terms of both water depth and velocity;
- different small-scale features (such as sewers, drainage systems, etc.), that were not considered in this thesis, are likely to produce significant effects in urban areas flooding scenarios;

- modifications of small-scale elements are relatively often, thus making difficult to maintaining the flooding model up to date;
- high-resolution models needs to be continuously updated in order to obtain durable, reliable results and to determine correctly the potentially floodable area, in the view of flood hazard assessment and management of local emergency plans;
- the question of costs connected to high-resolution surveys, the model set up and updating, still remains open, in addition to problems of over-parameterization and computational time;
- pure deterministic approaches do not face with modelling uncertainty, nor are suitable to be used in probabilistic framework (e.g., Montecarlo approaches), where multiple simulations have to be performed;
- the mesh resolution strongly depends on the objectives of the study. If the main objective is to have an overview of the flood dynamics, then a rough description of the street profile seems to be accurate enough. If an effective predictions of flood inundation extent and of the flow depth and velocity is required a high-resolution model, able to capture small-scale variation in topography, is essential;
- the main advantages of using coarse meshes lie both in simplifying the collection of topographical data and in reducing the calculation time, often prohibitive when trying to simulate precisely urban flooding.

Starting from the consideration that a high-resolution analysis is incompatible with a large-scale analysis, the second part of this thesis dealt with subgrid modeling, a technique that allows for the representation of the effects of urbanized areas in coarse grid, catchments scale applications.

Traditional method of representing structural features in a large-scale analysis usually involve upscaling of the roughness parameter that, in previous research, has been used as a key calibration parameter to compensate for the poorly represented momentum transfer process.

In the second part of the thesis, different tests for the same urban area have been carried out with various methods.

Attention was paid to:

i) the method ability to resolve the main flow field characteristics and, particularly, the preferential flow directions;
ii) verify the physical basement (and thus the practical applicability) of the approach;
iii) the predictive ability of the method;
iv) the computational resources requested.

A subgrid approach, already implemented in 2DEF hydrodynamic model, was found to account effectively for the global resistance of the urban area. However, this approach proved to be reliable only for quite isotropic urban areas, due to its inability to account for preferential pathways.

The classical method of upscaling of the roughness parameters has been analyzed, but the results were not even included in the thesis: the unreal variations of the resistance parameters and the necessity of heavy calibration cause the loss of model predictive skill.

A new method for subgrid modelling was developed and tested. This method is based on the concept of artificial porosity and takes into account anisotropic effects. Among the ones here explored, the anisotropic artificial porosity method is proven the most efficient and reliable approach to simulate the effects of urban areas in view of large-scale analysis, due to the following reasons:

- it results completely physical based and does not need the calibration of its parameters;
- it simultaneously reduces, with respect to traditional method, the needs of exceptionally high and unrealistic values of roughness parameter to represent the effects of urban structures, so that increasing the sensitivity of model predictions to the variation of the roughness parameter;
- it results the most accurate and reliable method, among the other tested, in term of agreement with the results obtained through high-resolution analyses, but also the most efficient in terms of computational time and the unique method that was able to guarantee an optimal predictive ability;
- it allows to model preferential flow paths in urban areas that arise from asymmetries in building shape or spacing, as well as from the alignment of buildings along streets;
- it offers significant predictive gain with little computational cost.

The good results obtained through the anisotropic, artificial porosity model is particularly encouraging. Particularly this method could lead to improved flooding forecasts in urban areas, simply relying on parameters that are calculated from topographical information, thus limiting the need of extensive calibration.

Bibliography

Defina A, D’Alpaos L, Matticchio B. A new set of equations for very shallow water and partially dry areas suitable to 2D numerical models. In: Molinaro P, Natale L, editors. Modelling flood propagation over initially dry areas. New York: American Society of Civil Engineers; 1994. p. 72–81.

Defina A. Two dimensional shallow flow equations for partially dry areas. Water Resour Res, 0043-1397 2000; 36(11):3251–64. http://dx.doi.org/10.1029/2000WR900167.

Defina A. Numerical experiments on bar growth. Water Resour Res 2003; 39(4):ESG21–ESG212. http://dx.doi.org/10.1029/2002WR001455.

D’Alpaos L, Defina A, Matticchio B. A coupled 2D and 1D finite element model for simulating tidal flow in the Venice channel network. In: Proceedings of the ninth international conference on finite elements in fluids, Venezia; 15–21 October 1995. p. 1397–406.

D’Alpaos L, Defina A. Mathematical modeling of tidal hydrodynamics in shallow lagoons: a review of open issues and applications to the Venice lagoon. Comput Geosci 2007;33:476–96. http://dx.doi.org/10.1016/j.cageo.2006.07.009.

Guinot V. Multiple porosity shallow water models for macroscopic modelling of urban floods. Advances in Water Resources. 2012: 37 p. 40-72

McMillan H.K, Brasington J. Reduced complexity strategies for modelling urban floodplain inundation, Geomorphology 2007: 90, p. 226-243

Mignot E, Paquier A, Haider S. Modeling floods in a dense urban area using 2D shallow water equations. Journal of hydrology 2006: 327, p. 186-199

Sanders B.F. et al. Integral formulation of shallow-water equations with anisotropic porosity for urban flood modelling. Journal of Hydrology 2008: 362, p. 19-38

Schubert J.E. et al. Unstructured mesh generation and landcover-based resistance for hydrodynamic modeling of urban flooding. Advances in Water Resources 2008: 31, p. 1603-1621

Yu D, Lane S. N. Urban fluvial flood modelling using a two-dimensional diffusion-wave treatment, part 1: mesh resolution effects. Hydrol. Process. 2006: 20, p. 1541-1565

Yu D, Lane S. N. Urban fluvial flood modelling using a two-dimensional diffusion-wave treatment, part 2: development of a subgrid-scale treatment. Hydrol. Process. 2006: 20, p. 1567-1583

Appendix A: Flow equations in 2D numerical model

Mathematical equations applied in the 2-DEF model are widely described in scientific literature (Defina et al., 1994; D'Alpaos et al., 1995; Defina, 2000; Defina, 2003; D'Alpaos & Defina, 2007). These equations are commonly used in many applications and are based on the solution of De Saint Venant equations in shallow water environment. De Saint Venant equations described free surface two-dimensional flow on the assumption of hydrostatic distribution of pressure, constant velocity along the vertical and fixed ground.

In particular, these equations are solved in 2DEF model adopting a numerical finite elements scheme in a triangular meshes used for schematizing the areas of interest. The system of two-dimensional shallow water equations consists of three equations: two equations for the conservation of momentum in the two orthogonal directions (A.1, A.2) and one equation for the continuity (A.3).

$$\frac{\partial h}{\partial x}+\frac{1}{gY}\frac{\partial q_x}{\partial t}+\frac{1}{gY}\frac{\partial}{\partial x}\left(\frac{q_x^2}{Y}\right)+\frac{1}{gY}\frac{\partial}{\partial y}\left(\frac{q_x q_y}{Y}\right)-\frac{1}{gY}\left(Re_{xx}+Re_{xy}\right)+\frac{\tau_{bx}}{yY}-\frac{\tau_{wx}}{yY}=0 \quad \text{(A.1)}$$

$$\frac{\partial h}{\partial y}+\frac{1}{gY}\frac{\partial q_y}{\partial t}+\frac{1}{gY}\frac{\partial}{\partial y}\left(\frac{q_y^2}{Y}\right)+\frac{1}{gY}\frac{\partial}{\partial x}\left(\frac{q_x q_y}{Y}\right)-\frac{1}{gY}\left(Re_{yy}+Re_{xy}\right)+\frac{\tau_{by}}{yY}-\frac{\tau_{wy}}{yY}=0 \quad \text{(A.2)}$$

$$\eta\frac{\partial h}{\partial t}+\frac{\partial q_x}{\partial x}+\frac{\partial q_y}{\partial y}=0 \quad \text{(A.3)}$$

Where h is free surface height, q_x and q_y are local flows obtain by multiplying the local depth for the respective average velocity along the vertical. The level Y represents the volume of water for unit area, g is the gravity acceleration, Re_{ij} are the Reynolds parameters representatives of turbulent stress along different directions, τ_{bi} is the bottom stress and τ_{wi} is the surface stress due to wind action (not considered in this thesis).

The bottom stress τ_b (used in the equations A.1 and A.2) is defined as:

$$\tau_b=\gamma\, Y\, j \quad \text{(A.4)}$$

Where the τ is the bed shear stress, γ is the water specific weight, Y represents the volume of water for a generic surface area and *j* is the linear hydraulic head loss.

For Gauckler Strickler equations:

$$v=k_s\, R_H^{2/3}\sqrt{j} \quad \text{(A.5)}$$

The hydraulic radius Rh is for definition equal to the ratio between the total cross sectional area and the wetted perimeter of the flow.

For shallow water is possible to calculate the hydraulic radius considering that the width of the cross-sectional area, call b, is larger than the water depth Y.

$$R_H \;=\; \lim_{\left\{\frac{b}{Y}\to\infty\right.}\frac{b\,Y}{2Y+b}=Y \quad \text{(A.6)}$$

From the equation (A.6) is possible to define R_H=Y. Substituting this result in Gauckler Strickler equation (A.5) and adjusting it is possible to obtain:

$$j = \frac{v^2}{k_S^2 \; Y^{\frac{4}{3}}} \tag{A.7}$$

Velocity can be defined as usual:

$$v = \frac{Q}{b\,Y} \;\; with\; q = \frac{Q}{b} \tag{A.8}$$

Combine previous equations (A.4), (A.7) and (A.8) is possible to obtain:

$$\frac{\tau_b}{\gamma\,Y} = \frac{|q|\;q}{k_S^2\; Y^{\frac{10}{3}}} \tag{A.9}$$

Applying the next relationship (A.10), where γ is the water specific weight, ρ is the water density and g is the gravitational acceleration, is possible to define the principal equation (A.11):

$$\gamma = \rho\; g \tag{A.10}$$

$$\frac{\tau_b}{\rho} = g\;Y\left(\frac{|q|}{k_S^2\; H^{10/3}}\right)q \tag{A.11}$$

The level H represent an equivalent water level introduced for described the effect of dissipative effect when the water depth is comparable with the irregularities of the ground. The level Y represents the volume of water for a generic surface area (m^3/m^2)

Appendix B: Wet dry transition

A major challenge in the development of 2D numerical models concerned the wet and dry transition and the velocity of propagation of the water front.

Talking about the propagation of a thin water front wave in natural terrain, the irregularities of surface are definitely essential. These irregularities create, in a certain area, the simultaneous presence of dry and wet conditions.

Clearly, not the whole heterogeneity, which characterizes the motion of water from a microscopic to a wide scale, can be simulated explicitly within a model. Far from being feasible from a computational point of view, such pure deterministic approach shown great intrinsic limitations.
Such details of the flow are usually not required, and the averaged macroscopic flow information is sufficient. Thus, the above problems can be partially overcome by setting up a phenomenological representation of the overall processes, based upon the few available data, to supply a more refined, statistically equivalent, description of the physics.

Generally, the height of the surface of an area domain is characterized by the topographic medium bottom height. Irregularities are not consider due to

topographic simplification necessary to collect data for a wide area. This simplification is useful for a water front propagation with a water level higher than the irregularities because model needs lower number of data. Otherwise, if water front have a level comparable to irregularities height of the surface, topographical data are not sufficient to simulate bottom friction losses and water volume collected by elements in a certain timestep.
Moreover, using for a generic mesh the medium bottom height means that the surface results completely flat. Transition from dry to wet area in average condition become instantaneous creating a series of numerical problems in the application of the water flow equations.

An innovative contribution of University of Padova researchers in wet-dry transition, applied for the first time in 2-DEF model, is to not consider constant the bottom level but insert a new condition inside the flow equations.
2-DEF model apply a subgrid model to bottom levels of every singular element. To overcome the limitation connected to irregularities simulation, the 2-DEF model assume that exist, for every generic element, an interval of depth in which, during the passage of water front wave, a mixed condition is possible during the transition from total dry to completely wet.

Roughness of surfaces are insert in the model thanks to a new parameter, defined as a length, that represent irregularities distribution on the surface of computational element.

The fundamental concept in this approach is that is possible to design the transition from dry to wet condition varying, inside computational elements, water volume capacity. From a different point of view, is possible to define the transition as the variation of available floodable surface depending from water depth related to total element surface. If the water depth is lower than the element minimum irregularities, the floodable area results zero. As water depth increase also floodable area increase. After water level get to maximum irregularities height all the surface results floodable. The parameter that control the amplitude of the process is define in the model as a_r. Physically this parameter represents the irregularities of the surface and is calculated as the difference of real surface maximum height and the average height derived from topographical data.

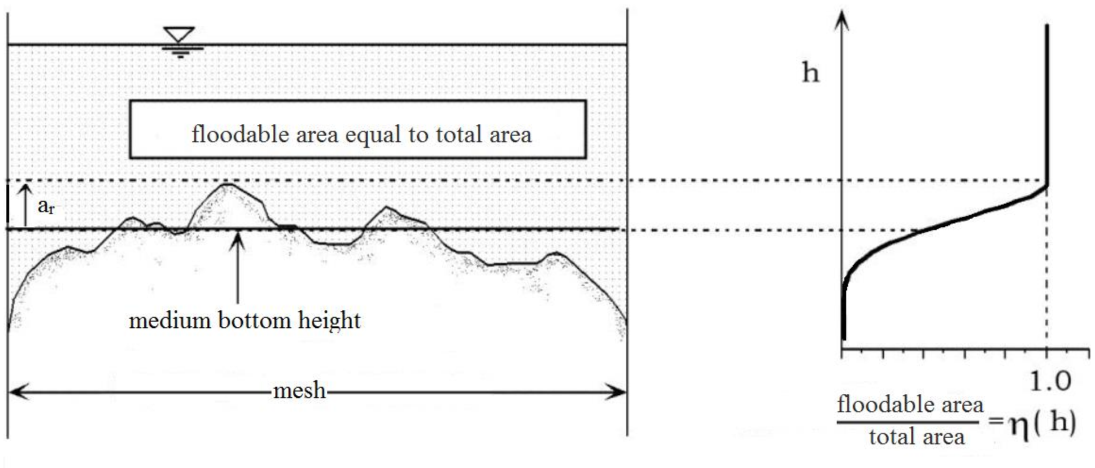

Figure B. 1 Bottom height schematic representation inside a computational element

Obviously, is impossible to determine manually the values of a_r for a generic soil. Consequently, was adopted a statistical approach where the bottom level is assumed to be distributed as a Gaussian probability function inside a certain area. This function have an average value h_f and a standard deviation σ_b that is a possible definition for the roughness of the bottom soil.

$$a_r = 2\sigma_b \tag{B.1}$$

Thus is assumed that the bottom level inside a generic area have a value included from +∞ and -∞ and so exist for every generic area at least a point that can be considered wet. Water depth, defined as water volume inside a specific area, due to this assumption cannot be equal to zero but only tend to zero if z tend to zero. The parameters used in the fundamental equation of 2DEF model described at page A-3 (equation A.11) is modified consequently:

$$\eta = \frac{1}{2}\left[1 - erf\left(\frac{2D}{a_r}\right)\right] \tag{B.2}$$

$$Y = \int_{-\infty}^{h} \eta dz = a_r\left(\eta\frac{D}{a_r} + \frac{1}{4\sqrt{\pi}}e^{-4\left(\frac{D}{a_r}\right)^2}\right) \tag{B.3}$$

$$H \cong Y + 0.27\sqrt{Y a_r}e^{-\frac{2Y}{a_r}} \tag{B.4}$$

Appendix C: "Urban area" two-dimensional special elements

In complex natural systems some particular hydrodynamics effects occurs. These effects could not be simply simulate, indeed would be required a very dense or very complex elements distribution. This problem is even greater if is considered a very large hydrographic basin. An example can be the river flow variation due to the presence of a structure instream, the flow volume decrease due to ground infiltration or the flow variation due to other particular hydraulic structures as dam, weirs, pumps and other. In these situations can be useful to add to certain elements, some additional equations or parameters that considered the processes in a general way.

In this thesis, special elements are used for modelling structures presence inside large-scale elements, like buildings, that are able to modify the flow paths. 2DEF model used special elements "maglie speciali fabbricato" to simulate the presence of buildings inside a defined area. In this manner, larger elements can be used for modelling complex urban area without needs of more specific mesh generation.

These special elements are used when, for computational or different problems, is impossible to include in the mesh grid all the buildings, even if properly simplified, present inside a specific area.

For the definition of this special element, two different aspects need to be analyzed. First, the continuity equation. The presence of buildings inside a mesh, in fact, reduce the total available flooded area for the water flow. Second, the total water flow resistance due to buildings presence.

For the continuity equation analysis, A_{tot} is defined as the total area inside a generic element (dashed line in Figure C. 1) and A_b as total area occupied by buildings.
Starting from this two plan areas is introduced a new parameter defined as buildings density:

$$\eta_b = \frac{A_b}{A_{tot}} \tag{C.1}$$

Is possible to define the parameter η as the percentage of free area available for water flow that can be utilized for continuity equation (A.3) defined in the Appendix A.

$$\eta = 1 - \eta_b \tag{C.2}$$

$$\eta \frac{\partial h}{\partial t} + \frac{\partial q_x}{\partial x} + \frac{\partial q_y}{\partial y} = 0 \tag{C.3}$$

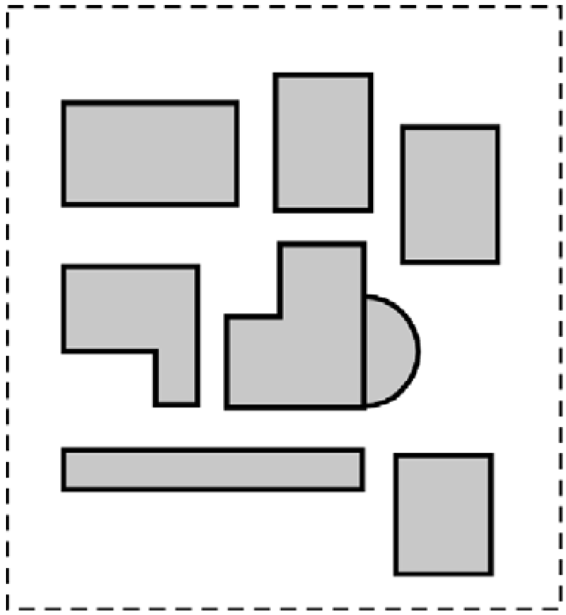

Figure C. 1 Urban area example for special elements definition

For dynamics effects, due to buildings flow resistance, is necessary to consider that the reduction of potential flooded area have an effect also for the level Y and H defined in Appendix A in the equation (A.11) and reported below.

$$\frac{\tau_b}{\rho} = g\, Y \left(\frac{|q|}{k_s^2\, H^{\frac{10}{3}}} \right) q \qquad \text{(C.4)}$$

Level Y represents the volume of water, for unit area, inside a generic mesh. The level H represent an equivalent water level. Defined as Y_o the hypothetical volume of water in buildings absence in a generic mesh, the real value of Y is:

$$Y = \frac{Y_o\, (A_{tot} - A_b)}{A_{tot}} = Y_0\, (1 - \eta_b) \qquad \text{(C.5)}$$

Similarly, with some approximation:

$$H = \frac{H_o\, (A_{tot} - A_b)}{A_{tot}} = H_0\, (1 - \eta_b) \qquad \text{(C.6)}$$

Finally, the equations (C.5) and (C.6) are insert in fundamental equation (C.4) for the definition of special element.

Considering dynamics aspects, is necessary to analyze other effects of flooded area reduction. First, needs to be considered flow resistance generated by water impact against buildings. In 2-DEF model, this effect is not considered because its contribution is negligible compared with other more important effect.

Second, needs to be considered buildings shielding effect. A given area behind a generic building is occupied by water with very low velocity that modified principal flow water path. Starting from this consideration is possible to assume that, from a dynamic point of view, the area not affected by water flow is greater than simple buildings area.

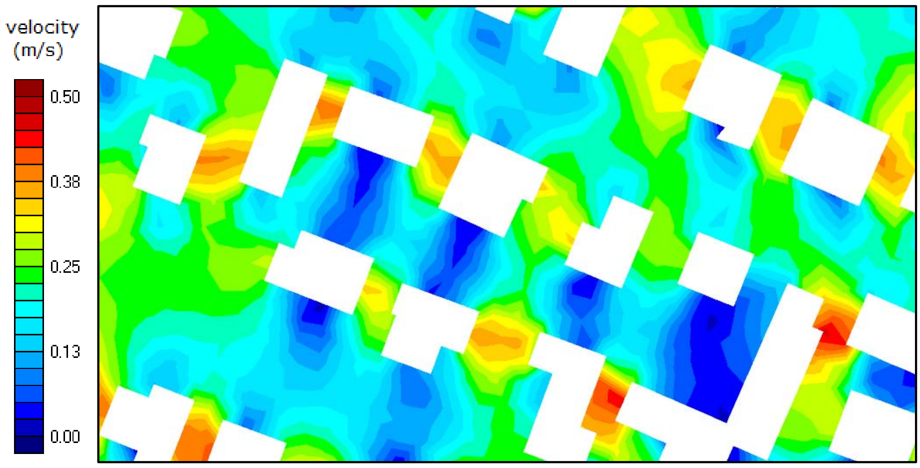

Figure C. 2 Velocity distribution zoom for shielding effect analysis

From Figure C. 2, in which buildings are singularly simulated, is possible to identify the blue areas where velocity is extremely low or equal to zero. This consideration have an important effect on H parameter for which is necessary provide an areal porosity greater than the areal porosity calculated only from buildings plan area. Defined as m_b the modified porosity, this parameter must be certainly greater than η_b and lower than 1 and must be substituted in place of η_b in equations (C.3).

From an analysis of Figure C. 2 is evident that areas not affected by water flow due to shielding effects cannot be easily calculated. New areal porosity call m_b, must be necessarily calibrated starting from the porosity η_b.

Third, needs to be considered path extension that water flow has to follow to pass through buildings area. This path extension is simulated in 2-DEF model as an equivalent reduction of Strickler roughness parameter.

Defined as L_b the ratio between water flow path, considering buildings presence, and water flow path in the absence of buildings, is possible to calculate the equivalent Strickler roughness parameter ks_{eq}:

$$\frac{k_{s\ eq}}{k_s} = \frac{1}{\sqrt{L_b}} \qquad \text{(C.7)}$$

Parameter L_b must be calibrated as porosity m_b. 2DEF model automatically calculate equivalent Strickler roughness parameter from L_b value.

Summarizing, 2DEF model needs three parameters for simulate buildings presence inside a certain mesh with special two-dimensional element: buildings density η_b, effective density m_b due to buildings shielding effects and length path parameter L.